# Method Development for Fatty Acid Analysis by Gas Chromatography with Nitrogen as Carrier Gas

By

Amena Alam Shanta

Thesis Submitted for the Degree of Erasmus Mundus Master's in Quality Management in Analytical Laboratories (EMQAL), Department of Chemistry, University of Bergen

Supervisor

Professor Svein A. Mjøs

October 2023

Bergen, Norway

# Acknowledgements

Above all, I want to thank the omnipotent God, who provides me with all I need and blesses me with positivity and willingness.

I would like to express my sincere gratitude to my supervisor, Professor Svein A. Mjøs, for his invaluable guidance and unwavering support throughout my thesis. His wise counsel, explicit study materials, and thorough training on how to apply MATLAB computer software for chromatography were vital in enabling me to complete my research. Professor Svein played a crucial role from the beginning of the project until the end, providing insightful comments and corrections that were instrumental in producing a high-quality thesis. Along with my personal experiences of dedication and persistence, this guidance has helped me acquire a deep understanding of chromatography and MATLAB.

I am deeply thankful to Professor Bjørn Grung for his valuable administrative support in helping me apply for a visa, arranging accommodation and providing me with other important resources. I am grateful to the chemistry department of the University of Bergen for accepting me as a student and granting me access to their lab facility to conduct my research project.

My appreciation belongs to the University of Barcelona, the institution that first admitted me as a student and where I completed all of the coursework for the master's degree. While at the University of Barcelona, I had access to numerous lab facilities and received encouragement from every professor there. I am deeply grateful to Professor Miguel Esteban Cortada and Professor Angeles Sahuquillo Estrugo for warmly welcoming me to Spain and providing their kind assistance and support throughout my stay at the university.

I am pleased to acknowledge the European Commission for providing the full funding. The EMQAL program creators and administrators have my deep gratitude. The program provided me with valuable education and connected me with students from around the world, allowing us to share our academic and social experiences.

Last but not least, I would like to dedicate this thesis to my family, who have always been there to support me.

# Contents

# Abbreviations

CCD--- Central Composite Design

DoE--- Design of Experiment

ECL--- Equivalent Chain Length

FAMEs--- Fatty Acid Methyl Esters

FID--- Flame Ionization Detector

GC---Gas Chromatography

H---Plate height

HETP (H)--- Height Equivalent to Theoretical Plate

ISO--- isothermal model detector

MS--- Mass Spectrometer detector

N ---Number of theoretical plates

PD--- Pressure drop

PEG---Polyethylene Glycol

PPC--- Peaks per Carbon

PTGC---Programmed temperature Gas Chromatography

RMSE---Root Mean Square Error

RMSEP--- Root Mean Square Error of Prediction

RSM--- Response Surface Methodology

SN --- Separation Number

VD--- Van Deemter equation / model

VD+Int --- Expanded van Deemter model (with interaction)

# Abstract

Retention indices are commonly applied to describe retention in gas chromatography. When analyzing fatty acid methyl esters (FAME), equivalent chain lengths (ECL) is the most common retention index system. Retention indices are used for peak identification, and the same stationary phase chemistry should provide the same retention index for a particular chemical. However, slight differences across columns of the same brand can cause retention indices to vary. Variations in column flow and temperature ramp rates also affect retention indices in temperature-programmed GC. These variations make it difficult to accurately reproduce retention patterns from one system to another, for example, when comparing systems with different carrier gases or column sizes.

The main objective of this study was to evaluate the effectiveness of transferring methods from helium to nitrogen carrier gas by assessing precise elution patterns and retention indices on four different capillary columns, BP20, DB23, BPX70 and IL111. The technique utilized response surface modeling and experimental design. Gas chromatographic parameters were systematically altered including carrier gas velocity, temperature ramp rate, and ramp start temperature. As a result, models were developed to predict ECL values based on chromatographic conditions.

The retention times were converted in ECL-values using saturated FAMEs for calibration. The retention patterns were similar in all columns with He and $N_2$ except IL111, which deviated slightly from the target patterns acquired with helium. When using $N_2$ and He, the chromatographic efficiency remained the same, but the retention times approximately doubled with $N_2$, as observed in BP20, DB23, and column IL111. BPX70 showed a horizontal transition, which was different from the other columns.

A quantitative study was conducted on 34 omega-3 capsules/supplements available in the European market. The study aimed to analyze the amount of the polyunsaturated fatty acids EPA, DPA and DHA in the samples. The mass percent for EPA, DPA and DHA were calculated for all the samples. BP20 column showed the best correlations between He and $N_2$ for EPA and DPA ($R^2$ = 0.999). In the case of DHA, the $R^2$ value was slightly lower (0.988). On the other hand, DB23 column gave the lowest $R^2$ value. For EPA, DPA and DHA, the $R^2$ values were 0.689, 0.573 and 0.872, respectively. The precision of the study was measured using relative standard deviation. All the nitrogen programs had RSD below 1%. With He, the maximum RSD was 0.99%, indicating

that all the columns produced precise results. The study demonstrated that it is possible to transfer retention patterns of FAMEs from He to $N_2$ after compromising between increased analysis time or loss in chromatographic efficiency.

# 1. Introduction

## 1.1. Fatty acids

A fatty acid from plants, animals, or microorganisms usually has a straight chain with an even number of carbon atoms, a carboxyl group at one end, and double bonds in the cis configuration in certain places relative to this [16]. Fatty acids (FA) that are crucial for nutrition, range in chain length from C12 to C24 and generally have 0-6 double bonds [4]. Common unbranched fatty acids are designated using the notation a:b n-c, where a and b stand for the fatty acid's number of carbon atoms and double bonds, respectively, and c stands for the position of the first double bond, as counted from the methyl end of carbon chain [4]. In nature, esterified forms of saturated fatty acids from animal and plant tissues can be discovered. They are consistently referred to as saturated hydrocarbons with the same number of carbons, but with the suffix -oic in lieu of the last -e [4].

In addition to being used to produce energy, fatty acids also help to construct biological membranes, which has an impact on the integrity, fluidity, permeability, and activity of enzymes that are membrane-bound. The kinds and quantities of fatty acids consumed as part of a normal diet have an impact on human health. Since they serve crucial physiologic functions in the body, the two classes of essential polyunsaturated fatty acids—omega-3 and omega-6—are linked to both healthy and unhealthy states. They are necessary since our body cannot produce them on its own and must rely completely on dietary intake. Numerous disorders, including coronary heart disease, hypertension, type 2 diabetes, rheumatoid arthritis, chronic obstructive pulmonary disease, and many others, have been linked to omega-3 fatty acids [1, 2]. They are known to also favorably influence behavioral problems and inflammatory illnesses [3]. Since the two categories of fatty acids have diametrically opposed metabolic effects, a healthy diet should include a good balance of omega-3 and omega-6 fatty acids. Blood viscosity, vasospasm, and a shorter bleeding time are all linked to high omega-6 fatty acid consumption [1].

Because of the beneficial effects of certain fatty acids, a large variety of fatty acid supplements are on the market. The supplements can be categorized into several groups based on the product labeling, the quantity of EPA and DHA in the items and principal component analysis of the whole

fatty acid profiles. One of the groups has typical "18/12 oils", which contain around 18% EPA and 12% DHA. The cod liver oils, and seal oils created two further dense clusters. The majority of the category comprises of goods that contain around 33% EPA and 23% DHA. As a result, they are referred to as "33/23 concentrates". Products were categorized as "high EPA products" or "high DHA products" depending on whether they contained more than 40% EPA or DHA [15].

## 1.2. Gas chromatography in fatty acid analysis

Gas chromatography is used for quantitative analysis of fatty acid composition. The fatty acids that are esterified in different lipid classes are converted into fatty acid methyl esters (FAME) before performing the gas chromatographic examination [11].

The hypothesis for a novel form of chromatography based on the partition of solute between two liquid phases was initially presented by Martin and Synge in 1941 [12]. Ten years later, James and Martin presented the first method for separating free fatty acids using gas-liquid partition chromatography [13]. Since then, the examination of volatile and thermally stable organic substances has typically been performed using gas chromatography. Open tubular capillary columns were introduced, which greatly increased separation power and enabled the analysis of complicated samples including hundreds of analytes.

The excellent capacity of contemporary capillary columns for the separation of complicated mixtures allows for the normal laboratory execution of GC studies of FAMEs. For the examination of FAMEs over a wide range of chain lengths and number of double bonds, there are several commercially available capillary columns designed specifically for the purpose. Over a packed column, capillary columns have benefits in terms of high-resolution capacity [14].

In gas chromatography, three carrier gases are in common use, which are Helium, Hydrogen and Nitrogen. Partly, because of the war in Ukraine, He is currently in short in supply. Moreover, He is expensive as it has limited reserve in the earth and hydrogen is explosive. As a result, in this study nitrogen is applied as carrier gas to minimize cost and tackle shortage of He.

## 1.3. Aims of the Study

The methodology applied in this work is based on the works of Mjøs and Waktola (2015), Waktola and Mjøs (2018) on separation efficiency, and the works of Chhaganlal et al. (2014) on selectivity and retention patterns [1, 17, 38]. The study is the attempt of combining these two methodologies in a development of a full method, where there is a lot of compromise between selectivity (retention pattern) and efficiency. The aim of this study is:

- To evaluate the use of nitrogen instead of helium as carrier gas for quantitative analyses of fatty acids
- To transfer GC methods for four different columns from He to $N_2$
- To characterize the properties of the four columns.
- To compare the performance of new methods ($N_2$) with the original methods (He)
- To compare quantitative data acquired with the new and original methods.

# 2. Theory

## 2.1. Gas chromatography (GC)

Gas chromatography (GC) is a crucial separation technique for identifying and quantifying compounds that are volatile. Helium, hydrogen, and nitrogen comprise the common mobile phases of GC, while solid or liquid stationary phases are either coated on the surface of the capillary column or supported by a solid support as solid stationary phases. The following is a list of the key components of gas chromatography: the sample injection system, gas supply, gas flow control, oven, and detector [10].

A conventional gas chromatograph has an injection system where samples are injected, a column where components are separated, and a detector where signals from the components that are eluted from the column are detected. The volatile solutes of a sample quickly partition between a stationary phase and a gaseous mobile phase (commonly referred to as carrier gas) when it is introduced into a gas chromatograph. The sample is fed into the column, where its constituent parts are separated depending on their distribution between the stationary phase and the mobile phase [19, 20, 21]. The retention factor, k, of the stationary phase in the equation represents the distribution of solutes between stationary phase and mobile phase.

Equation 1: $$k = \frac{amount\ of\ analyte\ in\ the\ stationary\ pahse}{amount\ of\ analyte\ in\ the\ mobile\ phase}$$

The time each molecule spend in the mobile phase is the same, and the degree to which the solutes are retained by the stationary phase varies and determines how the molecules separate. Temperature, stationary phase type, thickness, and column diameter are a few variables that might impact the retention factor [20]. Retention factor in isothermal gas chromatography, where the temperature remains constant during the run, may also be expressed in terms of adjusted retention times, $t_R$-$t_M$.

Equation 2: $$k = \frac{t_{R-t_M}}{t_M} = \frac{t'_R}{t_M}$$

Where $t_R$ is the retention time of a compound, which is the amount of time the compound needs from the moment the sample is introduced to the GC until the peak maximum appears. The amount

of time it takes for a non-retained compound to travel through the column is known as the hold-up time $t_M$, often known as "dead time." Adjusted retention time is the difference between a compound's retention time and the holdup time.

The objective of chromatography is to separate the components of the sample mixture into a sequence of chromatographic peaks, each of which represents a different component. Resolution ($R_S$), which is provided by [21], may be used to determine how far apart two chromatographic peaks A and B are from one another.

Equation 3: $$R_s = \frac{t_{R(B)} - t_{R(A)}}{0.5\left(w_{b(A)} + w_{b(B)}\right)} = \frac{\Delta t_R}{\bar{w}_b}$$

Where $w_{b(A)}$ and $w_{b(B)}$ are the corresponding peak widths at baseline of compounds A and B (where B elutes last), and $t_{R(A)}$ and $t_{R(B)}$ are the corresponding retention durations of compounds A and B, respectively.

If $R_S$ is raised, there is an increase in the resolution between the two peaks. This can be accomplished by either reducing the peak width or lengthening the distance between the two peaks. By raising the selectivity, which translates to an increase in the difference in retention between the solutes. The retention factor can be used to calculate chromatographic selectivity (α) or relative retention between two peaks as follows:

Equation 4: $$\alpha = \frac{k_B}{k_A}$$

Where and are retention factors of solute A and B, respectively.

The other way to improve resolution is to make the peak width smaller. When chromatographic separation first begins, solutes appear in narrow bands with a limited width. However, a phenomena known as band broadening will occur as the separation progresses in the column, widening the solutes' band. Column efficiency serves as a quantitative indicator of this peak broadening. A chromatographic column was defined by Martin and Synge as having distinct sections where the solutes are divided between the stationary phase and mobile phase [12]. Theoretical plates are these distinct chunks. Therefore, the number of theoretical plates (N) is the usual unit of measurement for chromatographic efficiency.

Equation 5: $$N = 16\left(\frac{t_R}{w_b}\right)^2$$

where $t_R$ and $w_b$ are the base peak width and retention duration of the peak under consideration, respectively. Equation 5 states that decreased peak widths or increased retention time (with the same peak widths) increases chromatographic efficiency. The number of theoretical plates depends on the length of the columns, L, and is thus connected to one another as follows:

Equation 6: $$H = \frac{L}{N}$$

The lower the value of H, the better the efficiency per meter column. H is also known as height equal to a theoretical plate (HETP). So, the goal of efficiency optimization is to reduce H.

One equation known as the Purnell equation condenses the three variables that affect the efficiency, selectivity, and retention of chromatographic separations.

Equation 7: $$R_s = \left(\frac{\sqrt{N_B}}{4}\right)\left(\frac{\alpha-1}{\alpha}\right)\left(\frac{k_B}{k_B+1}\right)$$

Where efficiency, selectivity, and retention are represented by the factors in the first, second, and third brackets, respectively. If we want to enhance our resolution, the equation informs us where to focus our efforts. It takes a column four times as long as the original to double resolution through N, while keeping all other variables constant. If poor resolution can be addressed via improving selectivity, it is typically the best option. Improving resolution through $k_B$ is only useful when $k_B$ is low.

## 2.2. Models of band broadening

The causes of chromatographic band widening are several. These three phenomena are the multiple route effect, longitudinal diffusion, and mass transfer resistance**.**

**Multiple paths:** As a solute passes through a packed column, it might take a number of alternative routes. As a result, the length of the path taken determines how long it takes the solute to elute out of the column. Band broadening results from this variance in elution time for solutes within the same band. This issue will be exacerbated by big particles and non-homogeneous packing.

**Longitudinal diffusion:** Because of net diffusion of analyte molecules from the center of a peak towards the edges, the chromatographic band widens. Reducing the amount of time the analytes

spend in the columns will reduce the effect of longitudinal diffusion, which in practice implies that the mobile phase velocity should be high to minimize this effect.

**Mass transfer:** Molecules are continuously exchanged between the mobile and stationary phases during mass transfer. But because the transition between the two phases is slow, molecules must first diffuse to the interface between the two phases before they can migrate from one to the other. The molecules in the mobile phase will migrate further down the column while some analyte molecules are stuck in the stationary phase, and how far they have travelled depends on the carrier gas velocity. As a result, this has a band-widening impact that grows with mobile phase velocity.

Van Deemter used all three components in his equation to define H as a function of carrier gas velocity (u) [21].

Equation 8: $$H = A + \frac{B}{u} + C \cdot u$$

The multiple route effect is described by the A term, the molecular diffusion of the solute in the mobile phase is described by the B term, and the barrier to solute mass transfer is described by the C term. Figure 2 shows how these three terms affect each other. The A term's contribution is unaffected by the velocity of the mobile phase. While the contribution from the C term grows with mobile phase velocity, the influence of the B term is stronger at low mobile phase velocity and subsequently rapidly declines as mobile phase velocity increases. An optimal velocity is the mobile phase speed at which the sum of the three terms is at its lowest value. The partial derivative of Equation 8 with respect to u is equal to zero at this point, since H has a minimum at optimal velocity. After determining the ideal velocity, $u_{opt}$ provides us with:

Equation 9: $$u_{\text{opt}} = \sqrt{\frac{B}{C}}$$

Since there is no column packing in capillary columns, the impact of band broadening caused by numerous routes should be absent. The Golay equation is produced by taking the A-term out of the van Deemter equation.

Equation 10: $$H = \frac{B}{u} + C \cdot u$$

The two most popular equations for explaining band broadening in chromatography are the van Deemter equation (Equation 8) and the Golay equation (Equation 10), however there are a number of alternatives and variations that, in certain cases, match data more accurately [22, 23, 24].

Throughout the column, the carrier gas's velocity, u, varies. The gas has a higher velocity at the end of the column than at the beginning because it can travel through the column by adding pressure and because gas may be compressed. As a result, the average carrier gas velocity is always meant. In his article for Journal of Chromatography A, L.M. Blumberg [22] showed the fallacy of the equations' form, which presumes H's dependency on a carrier gas' time-averaged linear velocity ($u = L/t_M$)

Due to compressibility of the carrier gas, Equation 10 is only accurate for systems with a very low pressure drop. For the higher pressure drops usually applied in modern GC, it is recommended to apply Equation 11 instead.

Equation 11: $H = \frac{B}{u^2} + C \cdot u^2$

## 2.3. Temperature programmed gas chromatography

As the oven temperature rises over time in temperature-programmed gas chromatography, a wider spectrum of volatile analytes may be analyzed than in isothermal GC.

Over the course of the study, this results in various solute-stationary phase and solute-mobile phase interactions. Equations based on the retention factor (k) are no longer useful in these circumstances since it changes. Since there is a connection between N and k, Equation 5 is likewise invalid. It is necessary to redefine selectivity and efficiency for temperature-programmed GC.

### 2.3.1. Selectivity in temperature-programmed GC

The concept of retention relative to a single standard substance became commonly used based on several ideas for how to use retention data from various published studies. The term "relative retention" is typically used to express this, and the idea is similar to what Equation 4 describes. But in temperature-programmed GC, these figures are highly system-dependent, particularly when the chemical characteristics of the analytes diverge sharply from the reference. Kovats' suggestion

of the so-called retention index system [25] was prompted by the challenge of having a single standard that is constantly close to the compounds of interest and the temperature dependence of relative retention. Retention index systems describe how the compounds of interest retain information in relation to a group of homologous benchmark substances. In order to calculate the retention index (I*x*) of any given material *x*, the formula shown below is applied in isothermal GC:

Equation 12: $$I_x = 100\left(\frac{\log t'_{R(x)} - \log t'_{R(z)}}{\log t'_{R(z+1)} - \log t'_{R(z)}}\right) + 100z$$

Where *x* is the target compound, *z* is an n-alkane with *z* carbon atoms eluting before the target compound, and *z*+1 is an n-alkane with *z*+1 carbon atoms eluting after the target compound [26]. For isothermal circumstances, use the aforementioned equation. A comparable approach that applies straight retention times without a logarithmic term or modifications is used in a linear temperature programme [27, 28].

Equation 13: $$I_x^T = 100\left(\frac{t_{R(x)} - t_{R(z)}}{t_{R(z+1)} - t_{R(z)}}\right) + 100z$$

where the remaining variables are the same as in Equation 12 above, and n is the difference in carbon number between the two n-alkanes used as a reference. This equation is often referred to as the van den Dool and Kratz equation [30].

The linear connection between the fatty acid methyl esters' (FAMEs') chain length (or "carbon number") and the logarithm of their retention period was also discovered by F. P. Woodford and C. M. Van Gent in 1960. They showed that unsaturated esters and esters with branching chains have nonintegral carbon numbers, whereas saturated esters also have integral carbon numbers [29]. Equivalent chain length (ECL), which appears to be derived from this "carbon number" idea, is used to characterize retention of fatty acid derivatives.

The reference chemicals are straight chain saturated fatty acid FAMEs. A version of the van den Dool and Kratz equation can be employed for a programmable temperature GC [30, 31, 32].

Equation 14: $$ECL_x^T = \left(\frac{t_{R(x)} - t_{R(z)}}{t_{R(z+1)} - t_{R(z)}}\right) + z$$

Where $t_{R(x)}$ is the retention time of compound x, $t_{R(z)}$ is the retention time of the saturated straight chain FAME eluting immediately before x, $t_{R(z+1)}$ is the retention time of a saturated straight chain

FAME eluting immediately after x, and z is the number of carbon atoms in the fatty acid chain of the saturated reference compound eluting before x (excluding the methyl group carbon in FAME).

## 2.3.3. Efficiency in temperature-programmed GC

Gas chromatography with temperature control cannot use N as a reliable indicator of efficiency. As a result, a different approach must be used. The separation number was initially used to express column performance by L. S. Ettre in 1975 [33]. The number of peaks separating two successive members of a homologous series is known as the separation number. It is written as the equation below:

Equation 15: $$SN = \frac{t_{R(z+1)} - t_{R(z)}}{w_{h(z+1)} + w_{h(z)}} - 1$$

Where $W_{h(Z)}$ and $W_{h(Z+1)}$ are the corresponding peak widths at half peak heights, $t_{R(Z)}$ and $t_{R(Z+1)}$ are the retention times of the two homologous series members with z and z+1 carbon numbers, respectively [9].

The inverse of SN is not a viable replacement for H since it approximates the number of peaks that can elute between two members of a homologous series. This is due to the fact that there is some separation efficiency even when SN is zero, since the homologues are still separated. Thus, the peak per carbon (PPC), a measure of the number of peaks that can be separated with chromatographic resolution equivalent to one per chemical in a homologous series, is utilized in this work as an alternative to SN. PPC may be calculated mathematically by dividing the average baseline peak width by the difference in retention times between the two homologous substances.

Equation 16: $$PPC = \frac{t_{R(z+1)} - t_{R(z)}}{0.5 \cdot (w_{b(z+1)} + w_{b(z)})} = \frac{t_{R(z+1)} - t_{R(z)}}{\bar{w}_{b(z,z+1)}}$$

If the retention and peak width are measured on a scale of retention indices, where the retention difference between homologous peaks is specified by definition (equal to 1 for equivalent chain lengths, ECL, and equal to 100 for Kovats indices), equation 16 is simplified to:

Equation 17: $$PPC = \frac{1}{w_{b,ECL}}$$

There is also a similar equation that relates SN to peak width in ECL units [36]. In a temperature programmed GC, peak width in retention index units should therefore be minimized to attain maximum efficiency, which is similar to minimizing H in isothermal GC. Finally, resolution ($R_s$), peak per carbon (PPC) and equivalent chain length (ECL) are related by the simple relationship:

Equation 18: $R_s = \Delta ECL \cdot PPC$

# 2.4. Optimization of efficiency and selectivity

The term "optimization" refers to the process of improving results in order to get a system to respond optimally [3]. In analytical chemistry, optimization refers to the discovery of the effects of changing a factor at a certain point of the experience in order to subsequently identify which conditions provide the optimal response.

## 2.4.1. Response surface methodology

Response surface methodology is a methodology in which response function(s) are obtained from experiments conducted in accordance to predetermined plan by varying the values of predictor variables. The predetermined plan is worked out by Design of Experiments (DoE). The response functions are typically polynomial models that link the response to the experimental settings and are obtained by regression [17]. For two variables system the model typically looks like:

Equation 19: $\hat{y} = b_0 + b_1 x_1 + b_2 x_2 + b_{12} x_1 x_2 + b_{11} x_1^2 + b_{22} x_2^2$

Where $x_1$ and $x_2$ represent the main effects, $x_1x_2$ represents the interaction and $x_{12}$ and $x_{22}$ represents the squared terms of the variables 1 and 2 respectively. The above model includes quadratic terms. Depending on the number of variables and their effect on the response the model may assume a higher order polynomial or a first order function where only the main effects and the interaction terms are included.

The efficiency in temperature-programmed GC was optimized using response surface methodology by Waktola [37]. In a temperature programed GC it is possible to assume that peak widths in retention index units (the inverse of efficiency) follow a response function of the two independent variables carrier gas velocity and temperature rate. However, the van Deemter

equation, which explains the inverse of the efficiency as a function of the carrier gas velocity, is not a quadratic function. Assuming that peak width in retention index units (w) follows the van Deemter equation with carrier gas velocity (u) and a function of temperature ramp rate (i), a response function that combines the two functions can be generated.

Equation 20: $$w_{\mathrm{b,ECL}} = a + \frac{b}{u} + c \cdot u + d \cdot i + e\frac{i}{u} + f \cdot i \cdot u$$

Where a, b and c-terms are the terms in the original van Deemter equation, d explains the linear effect of i on w, e explains the effect of i on the b-term in the van Deemter equation, and f explains the effect of i on the c-term in the van Deemter equation. This expansion of the van Deemter equation to account for an interaction will be referred to as a VD+Int model throughout the thesis. From the VD+Int model by inserting values for i it is possible to calculate ordinary VD models at any temperature ramp rate if the coefficients a-f are known. At an optimum velocity the partial derivative of Equation 20 with respect to u is equal to zero, since w has a local minimum at an optimum velocity value. One can therefore estimate $u_{\mathrm{opt}}$ at any temperature rate if the parameters b, c, e and f are known:

Equation 21: $$u_{\mathrm{opt}} = \sqrt{\frac{b+e\cdot i}{c+f\cdot i}}$$

## 2.4.2. Experimental designs

The experimental design approach is the foundation of the response surface technique [1]. There are several distinct experimental layouts. The number of experiments in the experimental setup varies substantially depending on the goal. The majority of designs, however, alter the predictor variables separately from one another, preventing correlations between the predictors. It is known as an orthogonal design [9].

**Factorial designs**

It is common practice to utilize factorial designs to study major effects and interactions. The designs are referred to as $2^k$ factorial designs when each component is modified across two levels. The number of variables examined is denoted by the letter k [9]. There are exactly $2^k$ experiments

required for a $2^k$ design. In experimental design, coded values are employed to make it easier to compare the relative relevance of the variables.

Each variable has a distinct physical scale; thus, all the variables are put on one common scale to facilitate the interpretation of significance for the various effects. The top level of a two-tiered design is coded as +1, and the lower level as -1 [8].

**Central composite design**

The central composite design is a popular design for chromatographic system optimization in place of expanding the factorial designs [5]. This design includes a two-level factorial design and extra axial points. The axial points and factorial points will both contribute to the estimation of the quadratic terms and the interaction terms, respectively [6]. At least one center point must be present in the design.

**Box–Behnken design**

Incomplete three-level factorial designs serve as the foundation for Box-Behnken designs. This may be represented graphically in two different ways: as a cube made up of the center and the middle points of the edges, or as a figure made up of three interlocking 2×2 factorial designs and a center point [7]. No factorial points or face points are present. The Box-Behnken designs should be employed when one is not interested in forecasting behavior at the extremes because they are not intended to be cubical designs [6, 2]. The interaction between all three elements ($x_1x_2x_3$) cannot be identified because one of the design variables in the Box-Behnken design for three factors always has the value zero.

**Doehlert design**

The Doehlert design is spherical for three variables and is not rotatable [2]. These designs benefit from features like high efficiency and little experimentation requirements [3]. The number of levels that may be explored in Doehlert designs varies depending on the issue. In order to extract the most information from the system, it is generally accepted that the variables having the strongest effects are investigated at the highest levels. Doehlert designs have regular intervals between the levels [3]. This design was used in both study of Waktola, 2015 and Chhaganlal [1,37].

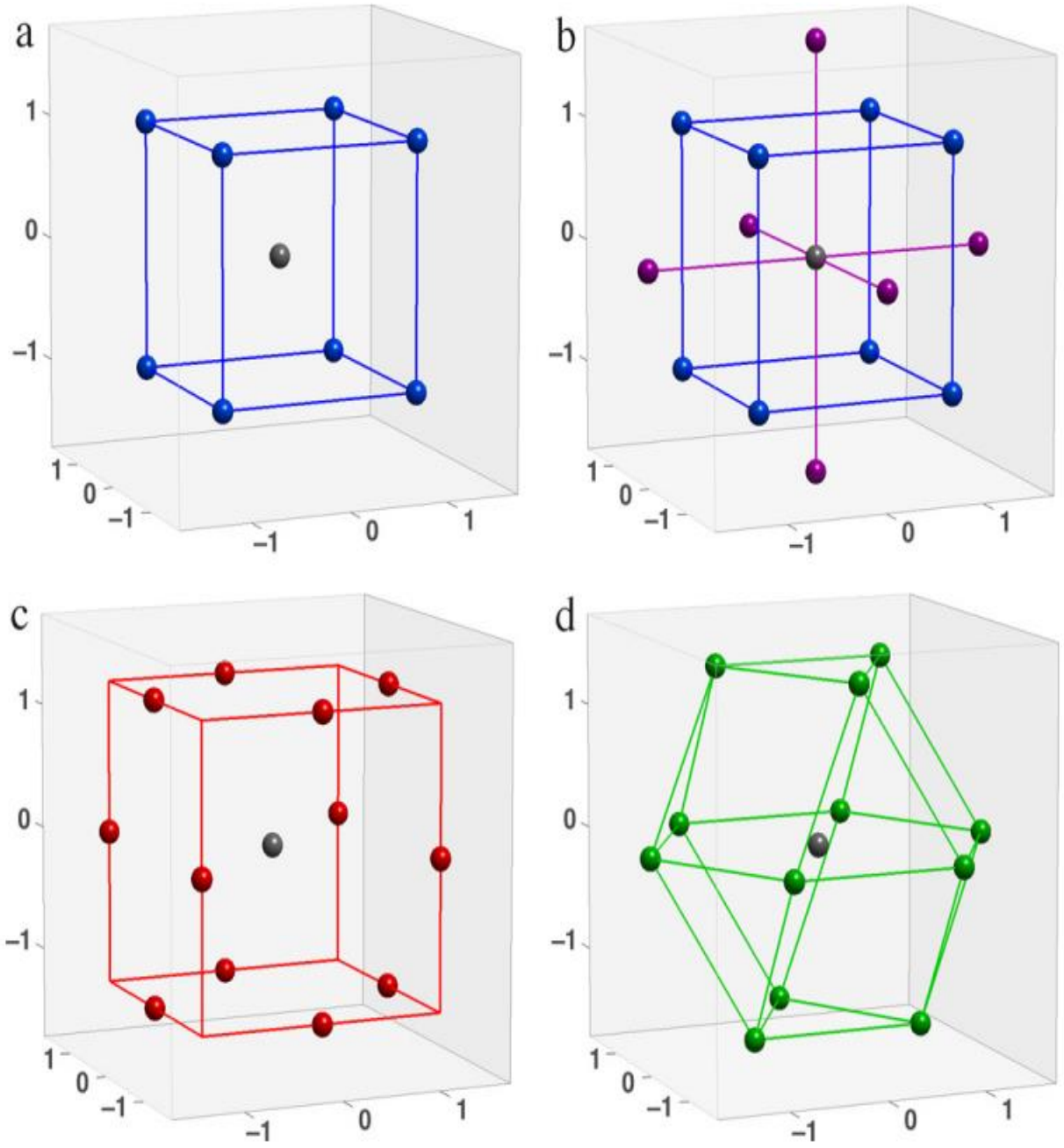


*Figure 1: Different experimental designs with three factors: full factorial design (a), central composite design (b), Box–Behnken design (c) and Doehlert design (d). The figures were generated by the Chrombox O software.*

## 2.5. Column chemistries

In gas chromatography (GC), choosing the right column is crucial to achieve precise and effective separations of the analytes in a sample. The degree of selectivity offered by various column chemistries varies, making it crucial to pick the proper column for certain fatty acid separations [34].

**Cyanopropyl (CP) Columns**

Cyanopropyl columns are a type of polar column, where a cyanopropyl functional group is linked to a silica support. CP columns can be particularly useful in the separation of cis- and trans-isomers when studying fatty acids. The polarity of the cyanopropyl stationary phase enables the preservation and separation of polar fatty acids based on variations in their chain length, double bond density, and number. However, the selectivity of CP columns may not be sufficient for separating fatty acids with highly similar structures [35].

**Polyethylene Glycol (PEG) /Wax Columns**

PEG/Wax columns are often used for fatty acid analysis due to their exceptional selectivity for polar molecules. These columns can effectively differentiate fatty acids based on their chain length, level of unsaturation, and placement of double bonds. The polar stationary phase interacts strongly with the functional groups present in fatty acids, resulting in well-defined peaks and high-resolution separations [35].

**Ionic Liquid (IL) Columns**

Ionic liquids used as the stationary phase in gas chromatographic columns give fatty acid analysis a special level of selectivity. Compared to conventional columns, ionic liquid phases interact differently with fatty acids, resulting in distinct separation patterns. These adaptable columns efficiently separate polar and nonpolar fatty acids [36].

For analyzing fatty acids in gas chromatography, the selectivity of the column is an important consideration. PEG/Wax and IL columns are often used due to their high selectivity and capacity for resolving a wide range of fatty acid isomers and structural variants. CP columns may also be useful for certain separations [36].

# 3. Experimental

## 3.1. Samples

This study includes 34 omega-3 capsules/supplements that span the variation in EPA and DHA composition in products on the European market. Omega-3 products that claimed to contain EPA, DPA and DHA were purchased from pharmacies or other retail locations in Norway (25 products), Italy (7 products), Spain (13 products), Germany (12 products), the UK (15 products), and France (1 product). Four other items were also ordered from Norwegian vendors online. The study samples are subsets of purchased samples. In order to avoid duplicates of the same product and brand name in the research, the products were chosen this way. However, it happens frequently that goods from the same producer are offered in other marketplaces under various product and brand names. Therefore, it is possible that several of the study's items used the same manufacturing method and starting materials. The day before analysis, the goods were removed out of the freezer where they were kept chilled at −20°C. When examined, every product was still within its shelf life.

## 3.2. Sample Preparation

### 3.2.1. Methylation reagents

The methylation reagent (Reagent 1) was dry HCl in methanol (2 M). 2M methanolic HCl were prepared by dilution of 3M methanolic HCl purchased from Supelco (Bellefonte, PA, USA, p/n 90964-100ML).

### 3.2.2. Direct Methylation

In a test tube 500 µL internal standard (approximately 4 mg/mL 23:0 FAME) was taken. Then all the solvent was evaporated by heating block and nitrogen (approximately 70°C). After completely drying the solvent, one drop of oil was added in the test tube and then the sample was weighed. After that, 1 mL methanolysis reagent (Approx 2 M dry HCl in methanol) was added to the test

tube. The top of the test tube was then filled with nitrogen and capped properly. Then the test tube was heated in oven at 90°C for 2 hours. Then half of the reagent in the test tube was evaporated at around 70°C. After that 1ml of distilled water and 1 ml of isooctane were added consecutively. The test tube was then vortexed for 30 s and centrifuged at 3500 rpm for 5 min. After centrifugation an isooctane layer was found, which was transferred to a 2 ml vial. The extraction step with 1 ml isooctane was repeated once (including vortexing and centrifugation) and the second extract was transferred to the same vial as the first. Finally, 5 μL of the combined extract was transferred to a GC vial that already contained 1 mL isooctane.

## 3.3. Reference Mixtures

**GLC793 Mixture:** GLC793 Mixture was applied for calculation of response factors and for optimization of retention patterns. This was bought from Nu-Chek Prep, and it contains equal amounts of the FAMEs (approx. 1.8 μg/mL in GC vials). The composition of the mixture is given in Table 1.

**Saturated FAME Mixture:** A mixture of saturated FAME was applied to calibrate the relationships between retention times and ECL values. This contained all saturated FAME from 12:0 to 28:0, excluding 13:0 and 23:0. FAME from 12:0 to 24:0 was purchased from Nu-Chek Prep, while 25:0 to 28:0 was purchased from Sigma-Aldrich. The concentration of each compound was approximately 0.9 μg/mL in GC vials. The composition of the mixture is given in Table 1.

**Mixtures for Efficiency:** Two additional mixtures were used for developing response surface models for efficiency. These consisted of a **Mixture-A** of saturated FAME (12:0 to 28:0, excluding 13:0, 23:0 and 25:0) and a **Mixture-B** of the unsaturated FAMEs given in the Table 1. The concentration of each compound was approximately 1.3 μg/mL in GC vials.

*Table 1: Reference mixtures used in the entire study.*

| GLC793 | Saturated FAME | Mixtures for Efficiency | |
|---|---|---|---|
| | | Mixtures-A | Mixtures-B |
| **12:0** | 12:0 | 12:0 | 16:1 n-7 |
| **14:0** | 14:0 | 14:0 | 18:1 n-9 |
| **14:1 n-5** | 15:0 | 15:0 | di-trans 18:2 n-6 |
| **15:0** | 16:0 | 16:0 | 18:3 n-6 |
| **16:0** | 17:0 | 17:0 | 20:3 n-6 |
| **16:1 n-7** | 18:0 | 18:0 | 20:5 n-3 |
| **17:0** | 19:0 | 19:0 | 22:6 n-3 |
| **17:1 n-7** | 20:0 | 20:0 | |
| **18:0** | 22:0 | 22:0 | |
| **18:1 n-9** | 24:0 | 24:0 | |
| **18:2 n-6** | 25:0 | 26:0 | |
| **18:3 n-6** | 26:0 | | |
| **18:3 n-3** | 27:0 | | |
| **20:0** | 28:0 | | |
| **20:1 n-9** | | | |
| **20:2 n-6** | | | |
| **20:3 n-6** | | | |
| **20:4 n-6** | | | |
| **20:3 n-3** | | | |
| **20:5 n-3** | | | |
| **22:0** | | | |
| **22:1 n-9** | | | |
| **23:0** | | | |
| **22:4 n-6** | | | |
| **22:5 n-3** | | | |
| **24:0** | | | |
| **22:6 n-3** | | | |
| **24:1 n-9** | | | |

## 3.4. Gas Chromatography

Two Agilent 7890A gas chromatographs were used for all studies. Both chromatographs were equipped with split/splitless injector, electronic pressure control, autosampler, and FID detector. Agilent Chemstation B.04.03 managed the GC systems. Injector and detector temperatures were 250°C and 300°C, respectively. Samples of 1 µl were injected splitless at 60°C where the temperature was held for 3 min before starting the temperature program. Methanol and isooctane were used to pre- and post-wash the injection needle. Helium and nitrogen were used as carrier gases, both were 99.999% pure. The mass flow of the carrier gas from the column remained constant during the chromatographic run since all tests were carried out in constant flow mode.

In reality, the carrier gas velocity constantly rises due to gas expansion as the oven temperature rises. Assuming that the actual column dimensions were the same as the nominal dimensions, the phrase "nominal carrier gas velocity" refers to the estimated average velocity at injection temperature (60°C). All velocities in the results section relate to nominal average velocities, which were calculated by the chromatographs' internal algorithm.

## 3.5. Capillary columns

Column: Gas chromatography on medium to highly polar stationary phases is generally used to analyze fatty acid methyl esters (FAME) [1]. The following GC columns in Table 2 were applied in the study.

*Table 2: Description of columns used in the study.*

| Column number | Column type | Stationary Phases | Dimension | | | Temperature limit ($^0$C) | Manufacturer |
|---|---|---|---|---|---|---|---|
| | | | L (m) | $d_c$ (mm) | $d_f$ (µm) | | |
| **1** | BPX70 | 70% Cyanopropyl Polysilphenylene-siloxane | 60 | 0.25 | 0.25 | 260 | SGE, Ringwood Australia, p/n 054623 |
| **2** | BPX70 | 70% Cyanopropyl Polysilphenylene-siloxane | 30 | 0.22 | 0.25 | 260 | SGE, Ringwood Australia, p/n 054612 |
| **3** | DB23 | (50% Cyanopropyl)-methylpolysiloxane | 30 | 0.25 | 0.25 | 260 | Agilent, Palo Alto, CA, USA, p/n 122-2332 |
| **4** | BP20 | Polyethylene-Glycol (PEG) | 30 | 0.25 | 0.25 | 260 | SGE, Ringwood Australia, p/n 054427 |
| **5** | SLB-IL111 | 1,9-Di(3-vinylimidazolium) nonane bis(trifluoromethylsulfonyl)imid | 30 | 0.25 | 0.2 | 270 | Supelco, Bellefonte, PA, USA, p/n 28927-U |

## 3.6. Chromatographic conditions

The conducted experiments can be divided into 2 steps:

The following programs were applied for initial quantitative studies with He as carrier gas:

- **BPX70 (60 m):** Oven temperature was 60°C for 3 min, then 60°C/min to 168.6°C followed by the main temperature rate of 1.448°C/min to 234°C. Carrier gas velocity at injection was 22 cm/sec. The program was tuned to match retention indices reported at www.chrombox.org.
- **DB23:** Oven temperature was 60°C for 3 min, then 60°C/min to 165°C followed by the main temperature rate of 2.9°C/min to 245°C. Carrier gas velocity at injection was 27.5 cm/sec. The program has been used on projects at the Department of Chemistry (UiB) but has never been published.
- **BP20:** Oven temperature was 60°C for 3 min, then 60°C/min to 160°C followed by the main temperature rate of 2°C/min to 250°C. Carrier gas velocity at injection was 26 cm/sec.

The program was based on the program for a similar column at Meier et al. (2006) but slightly adapted to fit a different column length and to resolve critical overlaps.

- **IL111:** Oven temperature was 60°C for 3 min, then 60°C/min to 144°C followed by the main temperature rate of 2°C/min to 190°C. Carrier gas velocity at injection was 26 cm/sec. The program was developed from scratch.

The final programs with $N_2$ as carrier gas were as follows:

- **BPX70 (30 m):** Oven temperature was 60°C for 3 min, then 60°C/min to 170°C followed by the main temperature rate of 1.0°C/min to 230°C. Carrier gas velocity at injection was 12 cm/sec.
- **DB23:** Oven temperature was 60°C for 3 min, then 60°C/min to 165°C followed by the main temperature rate of 1.3°C/min to 260°C. Carrier gas velocity at injection was 12 cm/sec.
- **BP20:** Oven temperature was 60°C for 3 min, then 60°C/min to 160°C followed by the main temperature rate of 1.0°C/min to 260°C. Carrier gas velocity at injection was 14 cm/sec.
- **IL111:** Oven temperature was 60°C for 3 min, then 60°C/min to 144°C followed by the main temperature rate of 1.0°C/min to 260°C. Carrier gas velocity at injection was 12 cm/sec.

## 3.7. Experimental designs

This study was conducted by applying a skewed experimental design similar to those applied in Desalegn (2018) [38].

The reason behind this are:

1) Optimal velocities tend to increase with temperature rate, and

2) The combination of the lowest velocities and highest rates will give too high elution temperatures to elute the last compounds.

On all columns, using the two carrier gases, the FAME samples were run at sixteen levels of carrier gas velocities and at four levels of temperature rates. Table 3 is a list of the carrier gas velocities

and temperature settings used. For all the columns under examination, the following general oven heating parameters were used: In order to ensure optimal analyte focusing, samples were injected at a column temperature of 60$^{o}$C and kept there for three minutes. The oven was then heated at a rate of 60$^{o}$C/min to reach the initial temperature of A$^{o}$C, and then at a rate of B$^{o}$C/min until elution of the final component. Table 3 provides a list of the experiments that were done.

*Table 3: List of experiments carried out on different columns studied.*

| **Experiment number** | **Temperature rate (°C/min)** | **Carrier gas velocity (cm/s)** | |
|---|---|---|---|
| | | **He** | **$N_2$** |
| **D01** | 1 | 8 | 8 |
| **D02** | 2 | 9 | 9 |
| **D03** | 3 | 10 | 10 |
| **D04** | 4 | 11 | 11 |
| **D05** | 1 | 12 | 12 |
| **D06** | 2 | 13 | 13 |
| **D07** | 3 | 14 | 14 |
| **D08** | 4 | 15 | 15 |
| **D09** | 1 | 16 | 16 |
| **D10** | 2 | 17 | 17 |
| **D11** | 3 | 18 | 18 |
| **D12** | 4 | 19 | 19 |
| **D13** | 1 | 20 | 20 |
| **D14** | 2 | 21 | 21 |
| **D15** | 3 | 22 | 22 |
| **D16** | 4 | 23 | 23 |

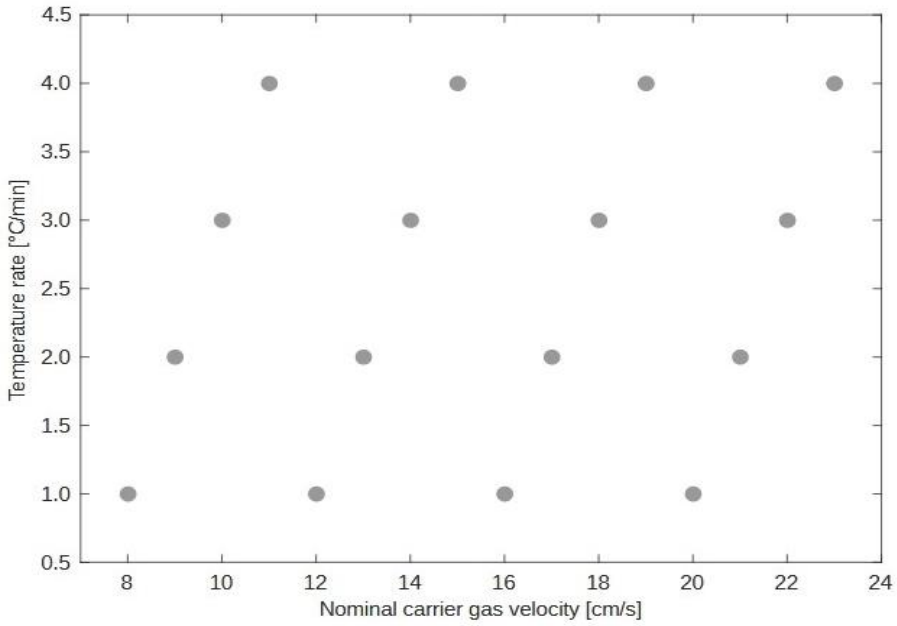


*Figure 2: The design used in temperature-programmed experiments.*

# 3.8. Chromatographic data handling

The study employed three separate Matlab-based programs. For the first treatment of GC-FID data, Chrombox C was utilized. The target surfaces were calculated, the response surface modeling, and the experimental design were all done using Chrombox Optimizer. The following is a brief summary of the key characteristics of the various software:

**Chrombox C**

Peaks are detected in samples using a template of retention indices. The samples are arranged in "boxes" which contain at least one calibration sample. The calibration sample is used to establish a link between retention times and the retention index scale. Samples that are obtained under identical conditions are placed in the same box. The other chromatograms in the box are then compared to this connection. This application is different from other software that uses retention indices, as the complete retention scale is transformed to retention indices. This enables the expression of peak widths on the scale of the retention index, which is useful for analyzing column efficiency (Equation 17). The SN can be calculated from the peak width of any peak in the chromatogram. Additionally, it is easy to investigate changes in retention indices using regression analysis, as the complete retention scale was converted to retention indices.

**Chrombox Q**

The initial purpose of Chrombox Q was to manage GC-MS data and arrange libraries of spectra and retention indices. The handling of retention indices is the same as in Chrombox C. Chrombox Q is available at www.chrombox.org/Q. In this work, Chrombox Q was used for creating the target ECL pattern for the BPX70 column.

**Chrombox Optimizer**

Since Optimizer enables reading data directly from the Chrombox C and Q, it is feasible to efficiently handle a large number of peaks. Optimizer eliminates the need for manual data entry, which reduces the overall time required for data handling. Since Optimizer directly extracts data from Chrombox C and Q, there is no chance of data entry errors while using it. The steps in an experiment are succinctly described below:

In the optimizer the experimental designs are initially set up.

- The GC is then used for experiments, and Chrombox C is used to process the chromatographic results.
- After that, the boxes from C are imported into the Optimizer, where each box from C (which typically contains several chromatograms) is given a distinct design point.
- While one or more target patterns (from Q or C) are simultaneously uploaded, none of the design points have been assigned to them. The peaks are recognized by both Q and C using a special identification code.
- When more than one peak has the same code in the box, the average value is utilized. Peaks can also be manually "passified" if necessary, for example if they are asymmetric, to ensure that they do not affect the average.
- Following the modeling of each individual surface, target surfaces are calculated using chosen targets and selected or all peaks.

The current version of Optimizer allows for two-dimensional (2D) designs to be modeled. The surface models used in Optimizer include the main effects, interactions between the two main effects, and squared terms of the main effects, in addition to the constant. The program also offers the option to create target models and surfaces by subtracting target values, which

explain the differences from the target or ideal conditions. You can find the latest version of Optimizer at: [http://www.chrombox.org/optimizer].

# 4. Result & Discussion

## 4.1. Characterization of columns and He programs

### 4.1.1. Elution temperatures

The elution temperature was measured at 24.0 and 22:6 n-3 in GLC samples and compared with upper temperature limit ($260^0$C) in all the four columns used in this study. Experimental conditions were D02 (9 cm/sec, $2^0$C/min) which is considered lower velocity and D14 (21 cm/sec, $2^0$C/min) which is considered higher velocity. There was no peak for 22:6 n-3 in BP20 column with lower velocity and that is why BP20 column was not compared for 22:6 n-3. Figure 3 shows elution temperature of 24.0 in GLC793 sample in different columns with $N_2$ gas.

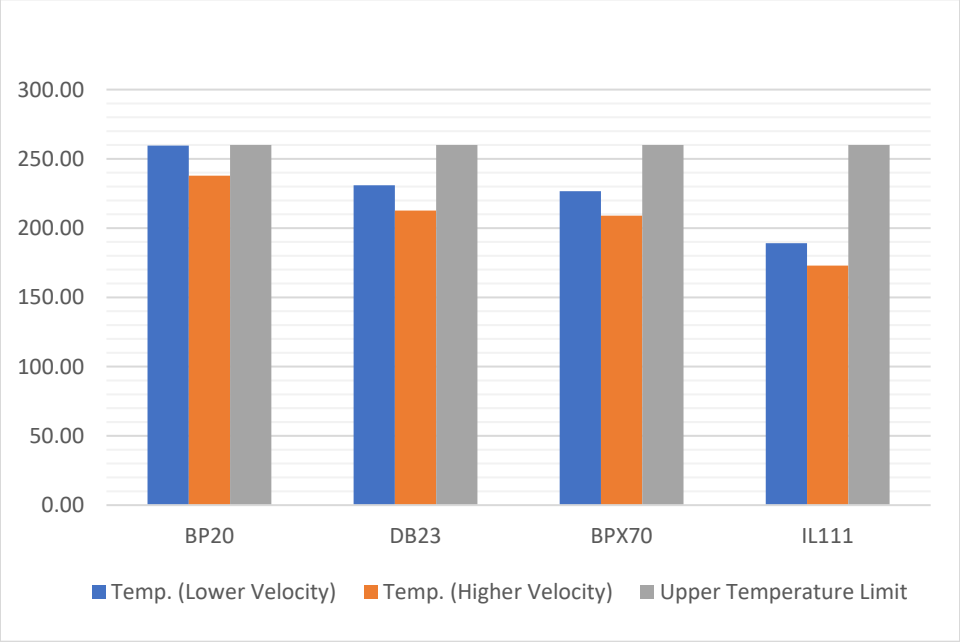


*Figure 3: Elution temperatures of 24:0 relative to upper temperature limit ($2^o$C/min, high and low velocity)*

From Figure 3, it can be seen that elution temperature of 24.0 is lower with higher velocity compared to elution temperature at lower velocity. The elution temperature was also compared with the upper temperature limit which is $260^0$C for all the columns. In BP20 column the elution temperature of 24.0 with lower velocity is almost same to the upper temperature limit. In contrast the difference between the temperate with lower velocity and upper temperature limit is highest in IL111. Increased oven temperature generally reduces the retention time of the compound. In Columns with the He gas, the retention times are much lower compared to retention times with $N_2$.

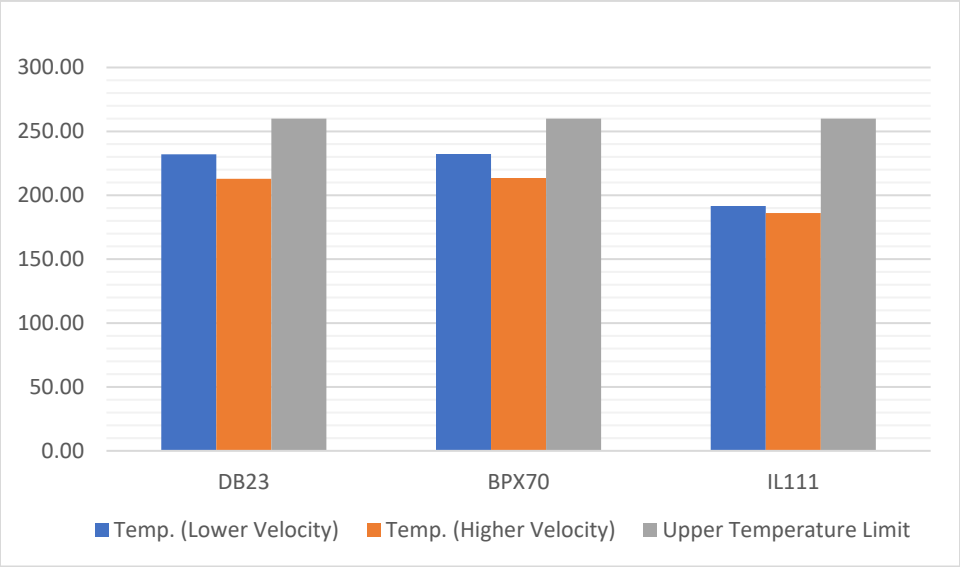


*Figure 4: Elution temperatures of 22:6 n-3 relative to upper temperature limit (2°C/min, high and low velocity)*

From Figure 4, it can be seen that elution temperature of 22:6 n-3 is lower with higher velocity compared to elution temperature at lower velocity. The elution temperature was also compared with the upper temperature limit which is $260^0$C for all the columns. The difference between the temperature with lower velocity and upper temperature limit is highest in IL111.

## 4.1.2. Column bleed

Column bleeds were observed on chromatograms taken from experiment D6 ($2^0$C/min, 13 cm/s with N2), but because the programs have different start temperatures, they are not identical. All programs covered the region $170^0$C to $250^0$C, and it is this region that is shown in the

chromatograms. Because the data has been acquired at different instruments and at different times, it is not possible to use the response from the detector directly. This is therefore normalized to the height of 18:3 n-6 in the GLC793 mixture (which is set to 100%). In addition, there will be a background signal from the detector. At low temperatures it can be assumed that there is no significant bleed and the signal at baseline is the background from the detector. The bleed at a certain point is therefore:

Equation 22: $$Bleed = 100 \frac{(\text{signal at the point of interest} - \text{the lowest signal in the chromatogram})}{\text{height of 18:3 n}-6}$$

The baseline signals have been measured at $250^0$C and at the baseline around the last eluting peak and both of these are important to consider.

DB23 shows highest column bleed at $250^0$C (73%) in contrast to BPX70, where column bleed is very low (11%). BP20 and IL111 have for instance similar bleed at $250^0$C, but the elution temperature for the last compound is more than $50^0$C lower on IL111 than BP20. At this point there is almost no background. So, it is not necessary to run IL111 in conditions where the bleed is significant. For BP20, the elution temperature of the last compound is above $250^0$C. This peak is therefore not shown in the chromatogram and the column bleed at the last peak is higher here among all the columns (32%). In IL111 column bleed is lowest which 0.5%.

From Figure 5, it can be seen that the elevated background in the beginning of the IL111 column is bleed from the previous chromatogram in the sequence. This is because of the carryover of bleed for IL111 but not for the other columns. 18:3 n-6 and the last peak (22:6 n-3) is marked in the chromatograms.

It should be emphasized that this is a rough comparison, but it is consistent with what is observed for the columns in general. The concentrations of GCL793 are approximate, since we use only 5uL when it was diluted. In addition, there are variations in the injected volume (1uL) on the GC. There are also minor differences in peak widths of 18:3 n-6, which will affect the peak height.

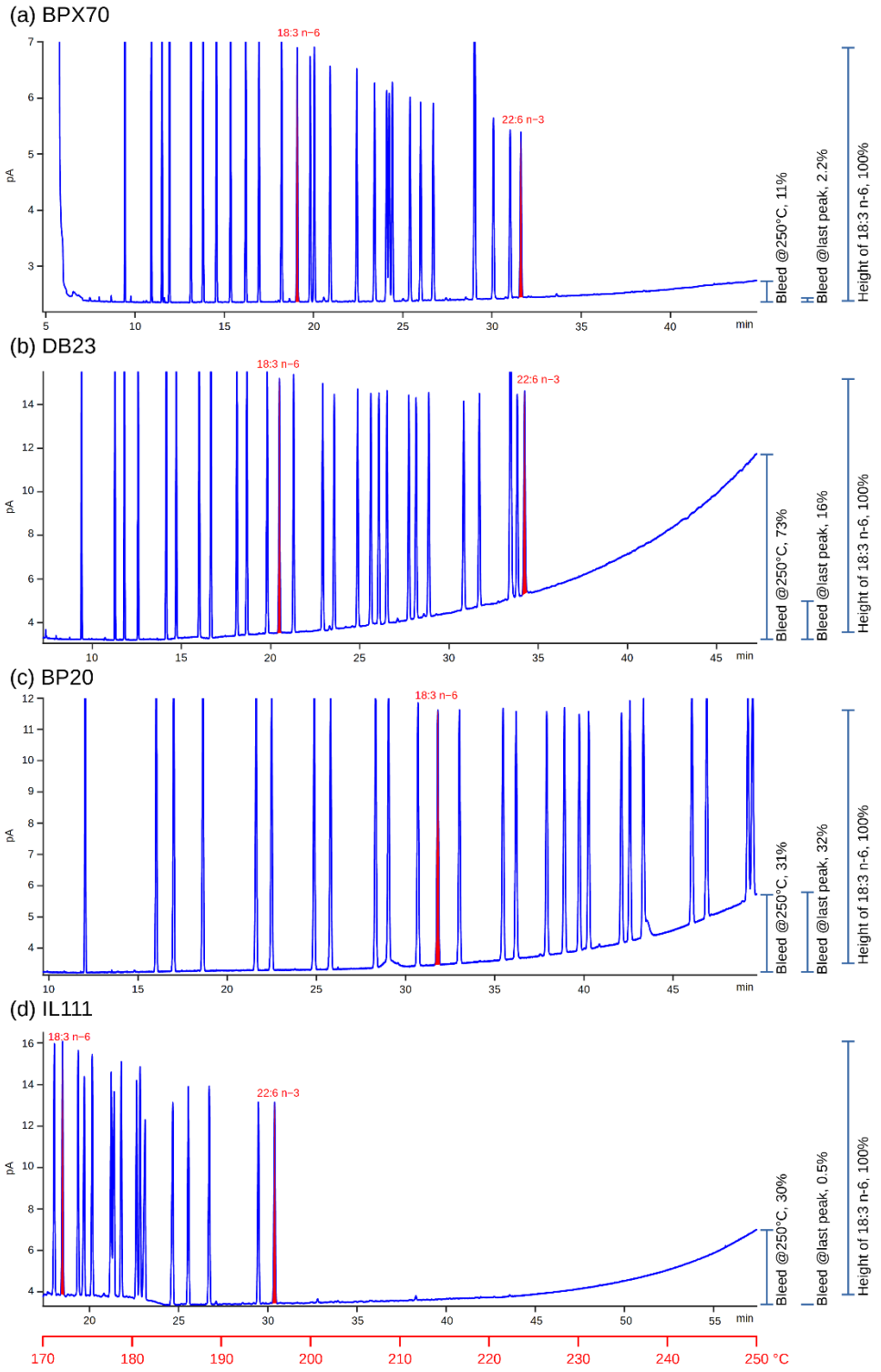


*Figure 5: Column bleed in the four columns.*

### 4.1.3. Column Polarity

The elution patterns of FAMEs are affected by the polarity of the stationary phase and also have some dependence on other chromatographic conditions, such as the applied temperatures. Figure 6 shows the elution pattern of FAMEs on the four columns with different polarities. The four-columns used in this study range from medium to high polarity. The two medium polarity columns are BP20 and DB23, one high polarity BPX70 and one ionic liquid column IL111 which is very highly polar. The columns are given in the order of increasing ECL values of unsaturated compounds and with ECL values as the retention scale. The differences in selectivity and polarity can be seen for instance by tracking 18:3 n-3, 20:5 n-3 and 22:6 n-3. 18:3 n-3 elutes around 19 ECL both in BP 20 and DB23. In contrast it elutes slightly before 20 in BPX70 column while it elutes just before 22 in IL111 column. In case 20:5 n-3 it is again the same in BP20 and DB23 where it elutes before 22. In BPX70 column, it elutes midway between 24:1 n-9 and 22:4 n-6. In BP20, 22:6 n-3 elutes after 24.0 and just before 24:1 n-9, while in DB23 it elutes just after 24.0. While in BPX70 and IL111 it elutes after 22:5 n-3 but there is difference in ECL values, which are 24.97 and 28.04, respectively.

Typical for polar columns is that retention increases with the degree of unsaturation. Retention also increases as the distance between the double bonds and the carboxyl group increases. An n-6 PUFA therefore elutes before its n-3 counterpart. The effect of the double bond position may be stronger than the effect of a single double bond [18].

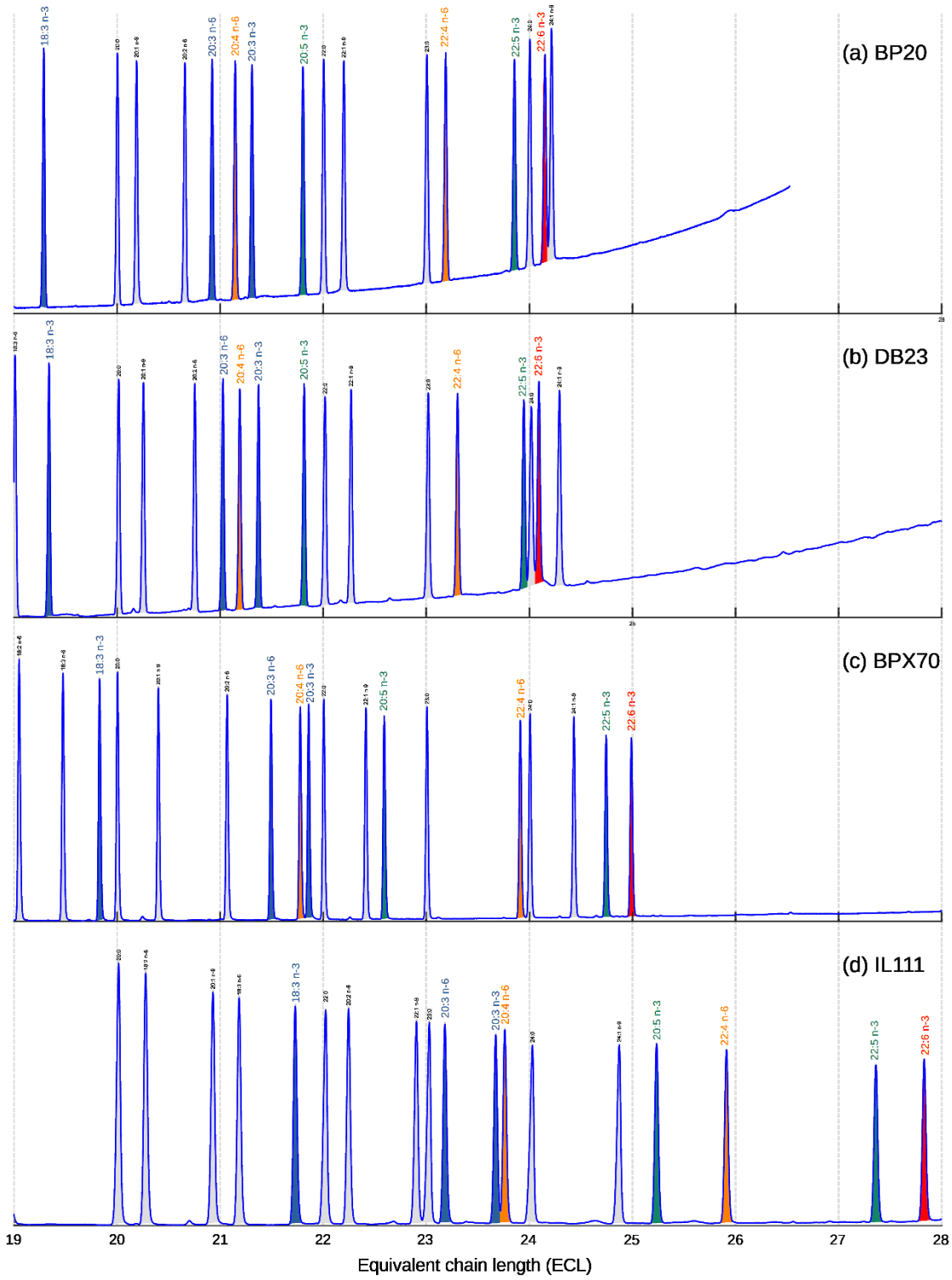


*Figure 6: Partial chromatograms of the GLC-793 reference mixture on ECL scale (19-28) on columns using the initial He programs, (a) BP20, (b) DB23, (c) BPX70 and (d) IL111.*

## 4.1.4. Shifts in polarity (ECL values)

The four-column used in this study ranges from medium to high polarity. The two medium polarity columns are BP20 and DB23, one high polarity BPX70 and one ionic liquid column IL111, which is very highly polar. The shifts in ECL values of 20:5 n-3 as function of carrier gas velocity and temperature rate are represented using response surfaces in the efficiency samples in Figure 7.

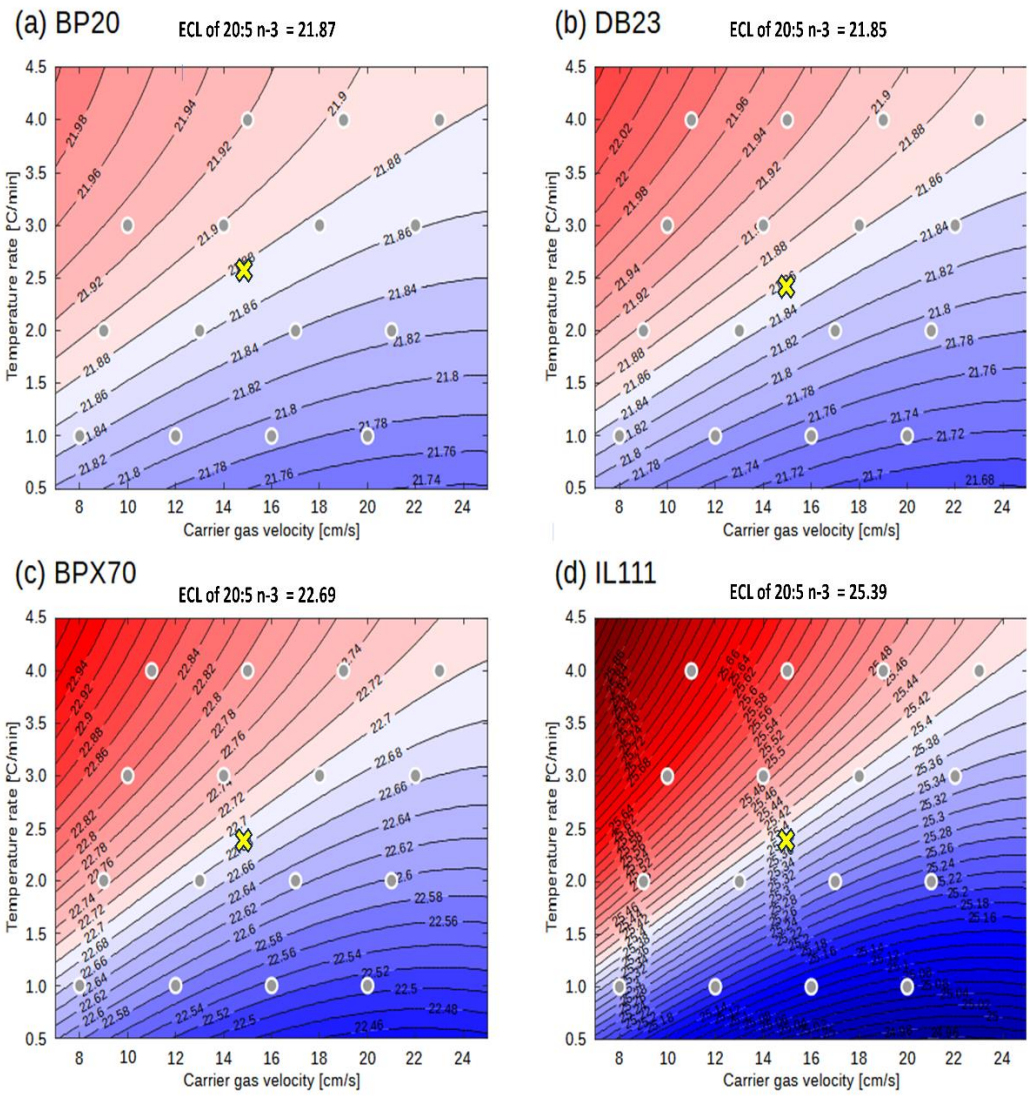


*Figure 7: The variation in ECL values of 20:5 n-3 on the columns as functions of the temperature rate and carrier gas velocity: (a) BP20, (b) DB23, (c) BPX70 and (d) IL111. Grey dots mark experimental conditions, and the yellow cross indicates the ECL of 20:5 n-3 in the original He programs.*

In Figure 7, all plots have the same color scale and the same distance between iso lines (Iso line spacing is 0.02 ECL units), so denser iso lines and stronger color indicate more shift. The experiments 13 cm/s -2$^0$C/min and 18 cm/s -3$^0$C/min are always close to the mean ECL, and the average ECL of these two is selected as the reference ECL with neutral (grey) color. Red and blue color indicate positive and negative deviations respectively. The color range in all plots are the same, the reference ECL value ± 0.5 (same deviation from the reference value should give same color). In all plots, 20 cm/s and 1$^0$C/min has the lowest ECL and 11 cm/s and 4$^0$C/min has the highest ECL which is presented below in Table 4.

*Table 4: Shifts of ECL values for 20:5 n-3.*

| **Columns** | **Min** | **Max** | **Range** |
|---|---|---|---|
| | **20 cm/s, 1 C/min** | **11 cm/s, 4 C/min** | |
| **BP20** | 21.77 | 21.95 | 0.18 |
| **DB23** | 21.73 | 21.98 | 0.25 |
| **BPX70** | 22.51 | 22.87 | 0.36 |
| **IL111** | 25.06 | 25.71 | 0.65 |

From Figure 7, it can be seen that the reference ECL values are higher in the column with high polarity. DB23 and BP20 have almost similar ECL in the reference point, where BPX70 and IL111 have higher ECL (22.69 and 25.29 respectively). Again, the shift of ECL values from negative to positive was also higher in the highly polar column. It is a tendency that the change in polarity with changing chromatographic conditions is highest for the most polar columns, which can be seen as smaller distances between the isolines. However, this is not a general trend without exceptions. For example, from the table it can be seen that DB23 has larger shifts in polarity than BP20, which is slightly more polar [17]. In contrast to IL111 which showed the highest range of shifts in ECL values. Large shifts in ECL values means that it is easier to alter the retention pattern (move the peaks relative to each other) by minor adjustments in temperature rate and carrier gas velocity. On the other hand, large shifts also mean that the patterns may be less stable (because columns change their properties over time) and may require frequent adjustments of the conditions to keep the optimal pattern. It is also more challenging to transfer methods between different systems.

### 4.1.5. Overlaps and closely eluting peaks

All original He programs had regions with closely eluting or overlapping peaks. A resolution of 1.5 is usually regarded as sufficient for accurate quantification, but one should ideally have some margins to this number to account for instabilities and changes of column properties over time. A 30-meter column used under normal operating condition typically gives PPC between 20 and 30 (with He) [17]. According to Equation 18, a delta ECL of 0.1 is required to give a resolution of 2 when the PPC is 20. Peak clusters with a separation of less than 0.1 ECL units are discussed below. From Figure 8, it can be seen that in BP20 22:6 n-3 elutes before 24:1 n-9 and overlaps with it where the difference in ECL values between them is only 0.06. DB23 column has similar elution patterns as BP20, but the overlap pattern is different.

In DB23 column 22:5 n-3, 24.0 and 22:6 n-3 overlap. In this case, the difference in ECL between 22:5 n-3 and 24.0 is 0.07. Again, the difference between 24.0 and 22:6 n-3 is 0.08. BPX70 and IL111 columns show some kind of similarity in overlap pattern.

In BPX 70 column two cases of closely eluting peaks can be seen; one is between 20:4 n-6 and 20:3 n-3, another is between 22:4 n-6 and 24.0. In the case of 20:4 n-6 and 20:3 n-3 the difference in ECL between then is 0.08. In the case of 22:4 n-6 and 24.0 the difference in ECL between then is 0.09.

The IL111 column shows more overlaps than other columns. Overlaps can be seen among 15.0 and 14:1 n-5, 17.0 and 16:1 n-7, 18.0 and 17:1 n-7, 22:1 n-9 and 23.0, 23.0 and 20:3 n-6, 20:3 n-3 and 20:4 n-6. The difference in ECL among them ranges from 0.07 to 0.24.

Although the peaks in the chromatograms shown in Figure 8 are separated well enough to be quantified by their area, the problem with closely eluting peaks becomes more severe in real samples where there are larger differences in peak height. The elution patterns in the figure are typical for what is used with these columns. Trying to resolve one peak overlap will typically create new overlaps.

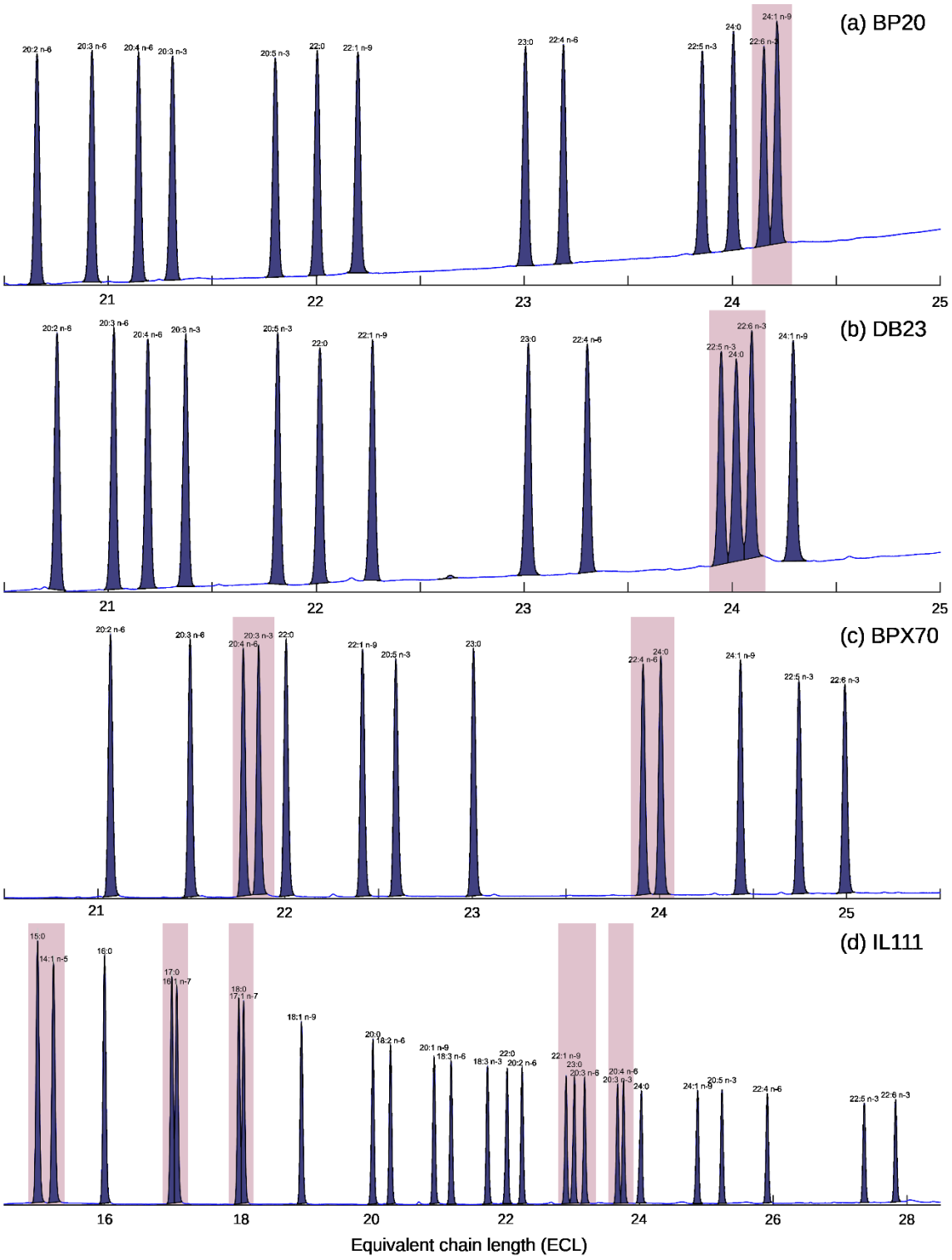


*Figure 8: Critical overlaps in all the columns with He as carrier gas.*

## 4.2. Development of the Nitrogen programs

### 4.2.1. Time of analysis

In a chromatographic analysis temperature rate and carrier gas velocity affects not only efficiency but also the time of analysis, which can be best expressed with the retention time of the last eluting compound. The shortest time of analysis is usually preferred, especially in a routine analysis of samples in a laboratory. There are combinations of carrier gas velocity and temperature rate that minimize the time for a required efficiency, or that maximize the efficiency that can be achieved within a certain amount of time. Evaluation of trade-off between time and efficiency is demonstrated in this section using all four types of columns and two types of carrier gases. The optimization process is demonstrated by using a full 4 x 4 design of the type illustrated in Figure 2.

**Models of retention time**

A model that appropriately describes the analysis time in terms of the retention time of the final eluting compound is required before evaluating the impact of temperature rate and carrier gas velocity on analysis time as well as determining the time efficiency trade-off. Both the carrier gas velocity and the temperature rate affect retention time. Retention time is reduced when one or both of the two components are increased. This study applied the retention time model developed by Waktola, 2015 [37]. The model was developed by conducting an experiment on 60 m BPX70 column and that was the only experiment which was performed on four levels of temperature rate. The developed model of retention time is given below-

Equation 23: $\ln(t_R) = D + E\ln(u) + F\ln(i) + G\ln(u)\ln(i)$

Where $t_R$ denotes retention time for the last eluting compound, $u$ for the velocity of the carrier gas, $i$ for the temperature ramp rate, and A, B, C, and D for the coefficients. To avoid the logarithmic form, the exponent of the equation was taken to produce a response surface that directly describes the retention time as a function of $u$ and $i$ once the model was developed and the parameters identified.

By using Equation 23, a response surface of the retention duration of the final eluting FAME which is the methyl ester of the saturated fatty acid of 24.0 was produced in all the four columns (Figure 9) in the original form of measurements of the parameters. In case of BP20 column experiments 3, 4 and 8 are excluded in the time model, since 24:0 did not elute under these conditions.

From Figure 9, it can be seen that, shorter retention times are attained at greater temperature rates and at higher carrier gas velocities in all the columns. Additionally, it has been found that in all the columns, increasing carrier gas velocity has a lesser impact than raising temperature rate. Although the relation of temperate and retention time is similar in all the columns, IL111 has the lowest retention time with the highest temperature rate in contrast to BP20 column, which has the highest retention time.

The goal of the analyst is to obtain analytical results as quickly as feasible. However, it is possible to get a lower retention time with the loss of efficiency. Therefore, we must assess the efficiency at all combinations of the temperature rate and carrier gas velocities used to derive the retention time model in order to determine the shortest time that may be attained.

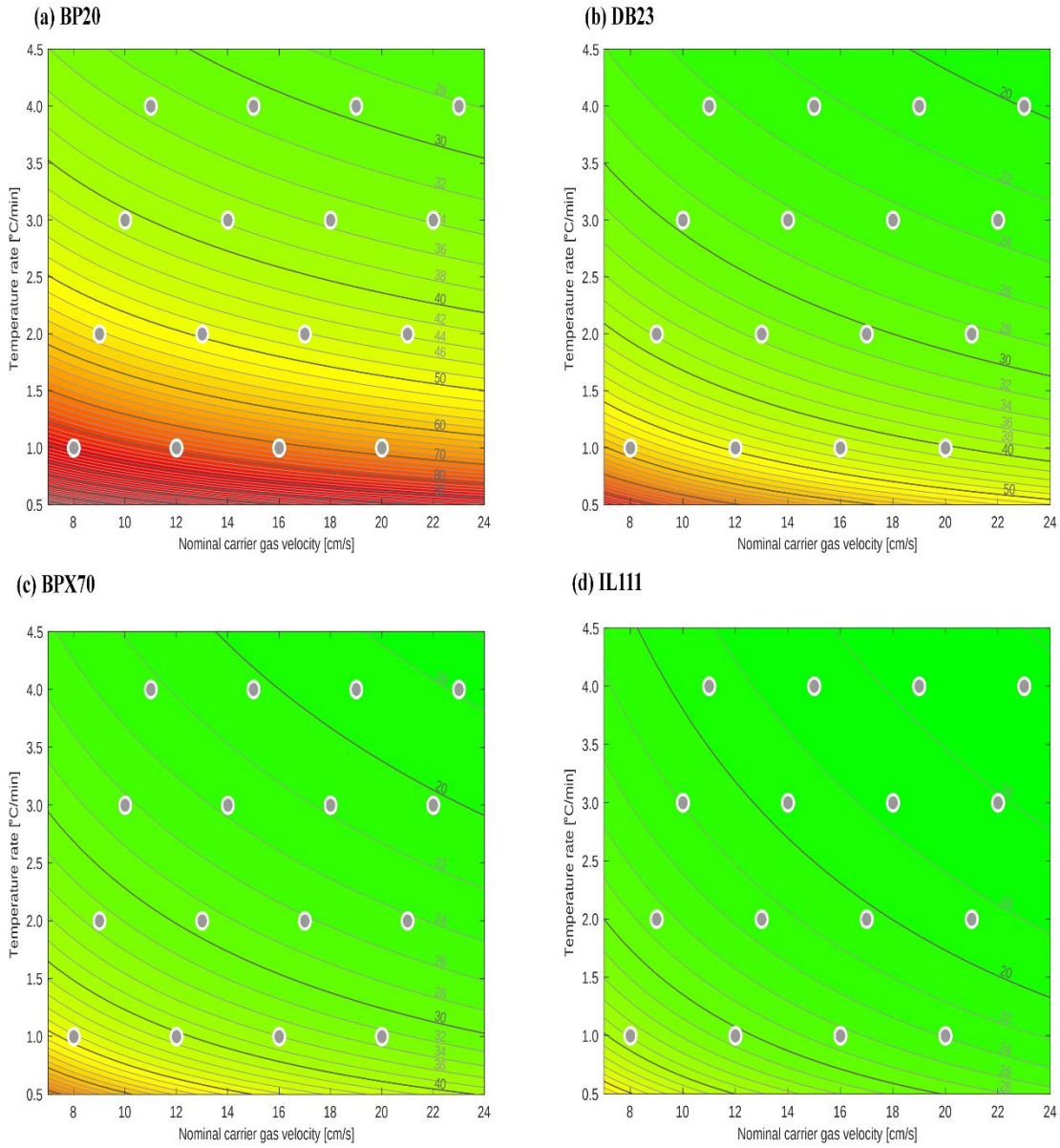


*Figure 9: Response surface plot of the retention time in minutes of the last eluting FAME (24.0), column: (a) BP20, (b) DB23, (c) BPX70 and (d) IL111, Nitrogen as carrier gas. Numbers on iso-lines represent retention time in minutes and the color scale is 14 (fully green) to 88 (fully red) minutes. Errors for the models are given in Appendix A1.*

## 4.2.2. Efficiency

The efficiency plots were created using Equation 20. In efficiency response plot, 12:0, 14:0 and 26:0 was excluded from the models because of asymmetry on some columns. For BP20, program

2, 3, 4, 5, 7, 8, 12 were also excluded in the model for 22:6 n-3 and program 3, 4, 8 were also excluded in the model for 24:0.

In the Figure 10, the black curves isolines indicate the response surface and ash color dots indicate experimental conditions. The black line passing through the iso-lines indicates optimal efficiency.

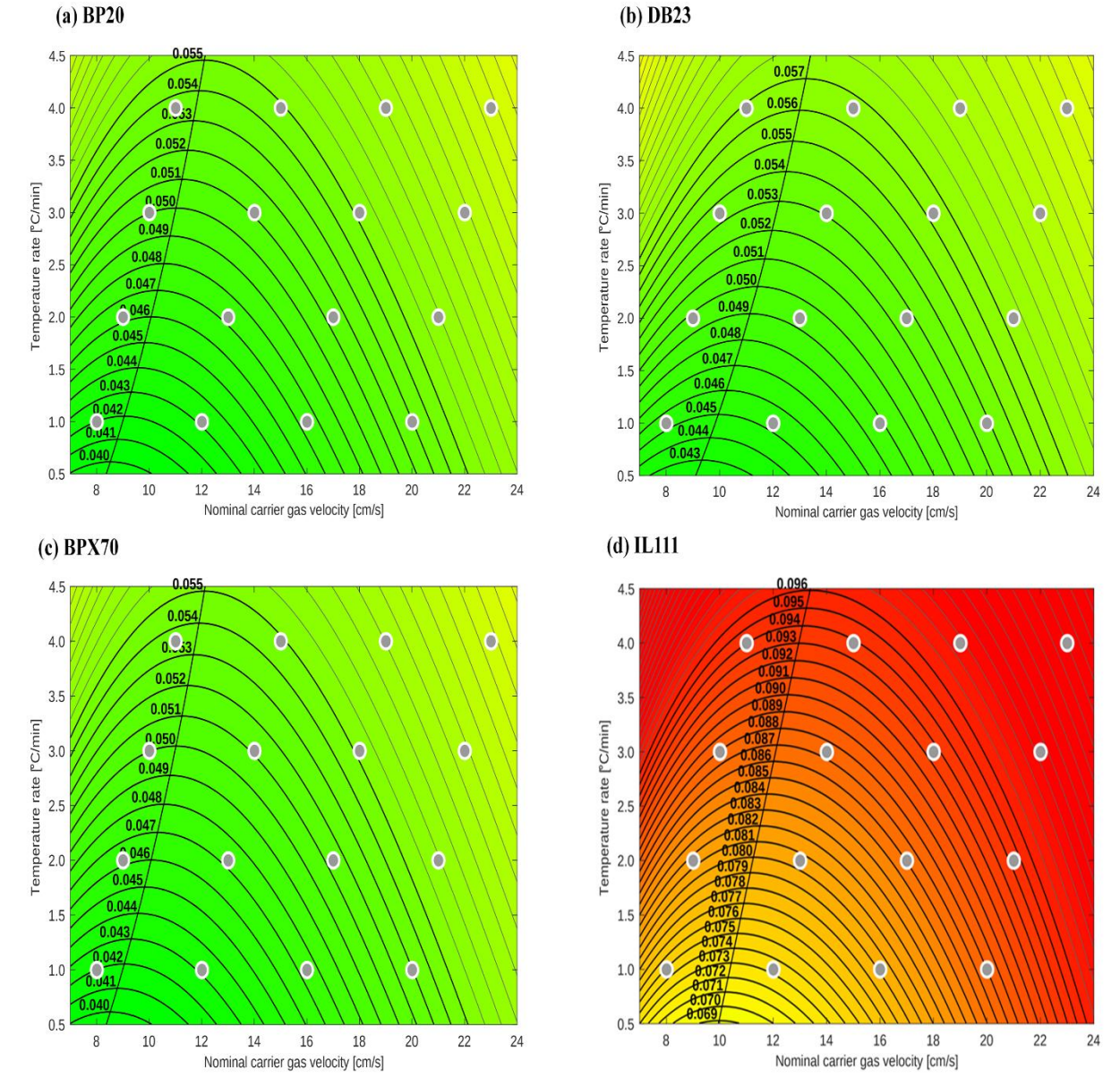


*Figure 10: Response surface plot of the efficiency of the last eluting FAME (24.0), on column: (a) BP20, (b) DB23, (c) BPX70 and (d) IL111, Nitrogen as carrier gas (Average deviation below 0.01 ECL units). The color scale is from 0.04 (fully green) to 0.1 (fully red). Errors for the models are given in Appendix A2.*

### 4.2.3. Time-efficiency trade-off

It is crucial to first combine the response surfaces for retention time and efficiency to comprehend the relationship between the two responses before attempting to explain the time efficiency trade-off. The retention time response plot (Figure 9) and the efficiency response plot (Figure 10) overlap is shown in Figure 11. The blue lines crossing the plots are the optimal velocity lines, which represent the minimum peak width or the maximum efficiency that can be achieved at a given temperature rate (Equation 21). The highest efficiency is found at lower temperature rates and ideal carrier gas velocities, but the shortest analysis time is found at higher temperature rates and higher carrier gas velocities, as can be seen from the overlapping surface plots. This indicates that if we are ready to wait for a longer length of time to complete the analysis, we can achieve better efficiency; alternatively, if we are willing to tolerate lower efficiency, we may complete the analysis of our sample in a shorter amount of time. However, it is undesirable to have a longer analysis time as well as less efficiency. Therefore, we must strike a balance between the amount of analytical time we can afford and the required degree of efficiency.

An iterative technique was used to determine the locations on the plot where the optimal time efficiency trade-off might be found [17]. The approach follows the iso-lines for the VD+Int model and derives the conditions that minimize the retention time on the iso-lines from the retention time model. The black points on the response surface correspond to these. After that, a spline function is fitted to the points and shown by the black line. The ideal circumstances for the trade-off between time and efficiency are shown by this line. One might argue that for every condition that is not along the black line, the same efficiency can be reached with less time spent on analysis or that efficiency can be improved with the same amount of time (Figure 11).

This line shows the ideal carrier gas velocity and temperature rate for the optimal tradeoff. The decision-making point along the line depends on how much efficiency is required or how much analysis time is acceptable. Time optimum velocities, or $u_{topt}$, are the conditions along this line.

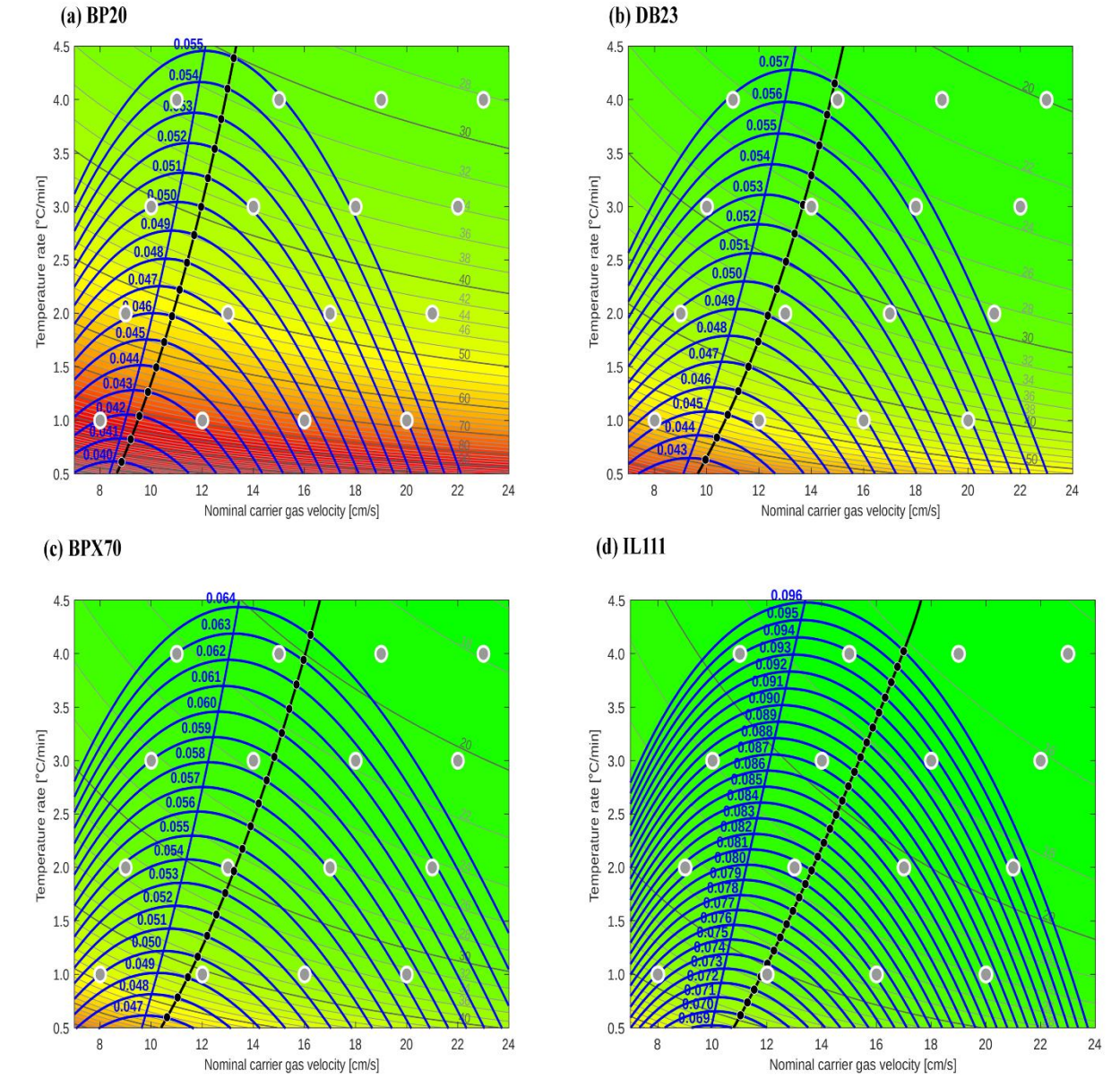


*Figure 11: Response surface plots showing best line of efficiency/time trade-off (the black line) in Nitrogen, column: (a) BP20, (b) DB23, (c) BPX70 and (d) IL111.*

## 4.2.4. Selectivity studies

Final selection of quantification of sample with nitrogen was done after combining efficiency and selectivity plots.

The selectivity plots were created using Equation 19. For BP20, 22:5 n-3, 22:6 n-3 and 24:1 n-9 are excluded from the models, since they eluted with few programs on this column. In the Figure

12 the dark green area shows the area where the average deviation from the target values from the helium program is lowest (<0.01 ECL units). Experimental conditions in this area will give best selectivity, i.e. the best reproduction of the retention patterns achieved with the corresponding He methods.

In Figure 12, the color scale is from 0.01 (fully green) to 0.1 (fully red). The dark green area marks where the average deviation from the target values is below 0.01 ECL units. Iso lines higher than 0.1 are not labeled as these conditions give results very far from the target pattern.

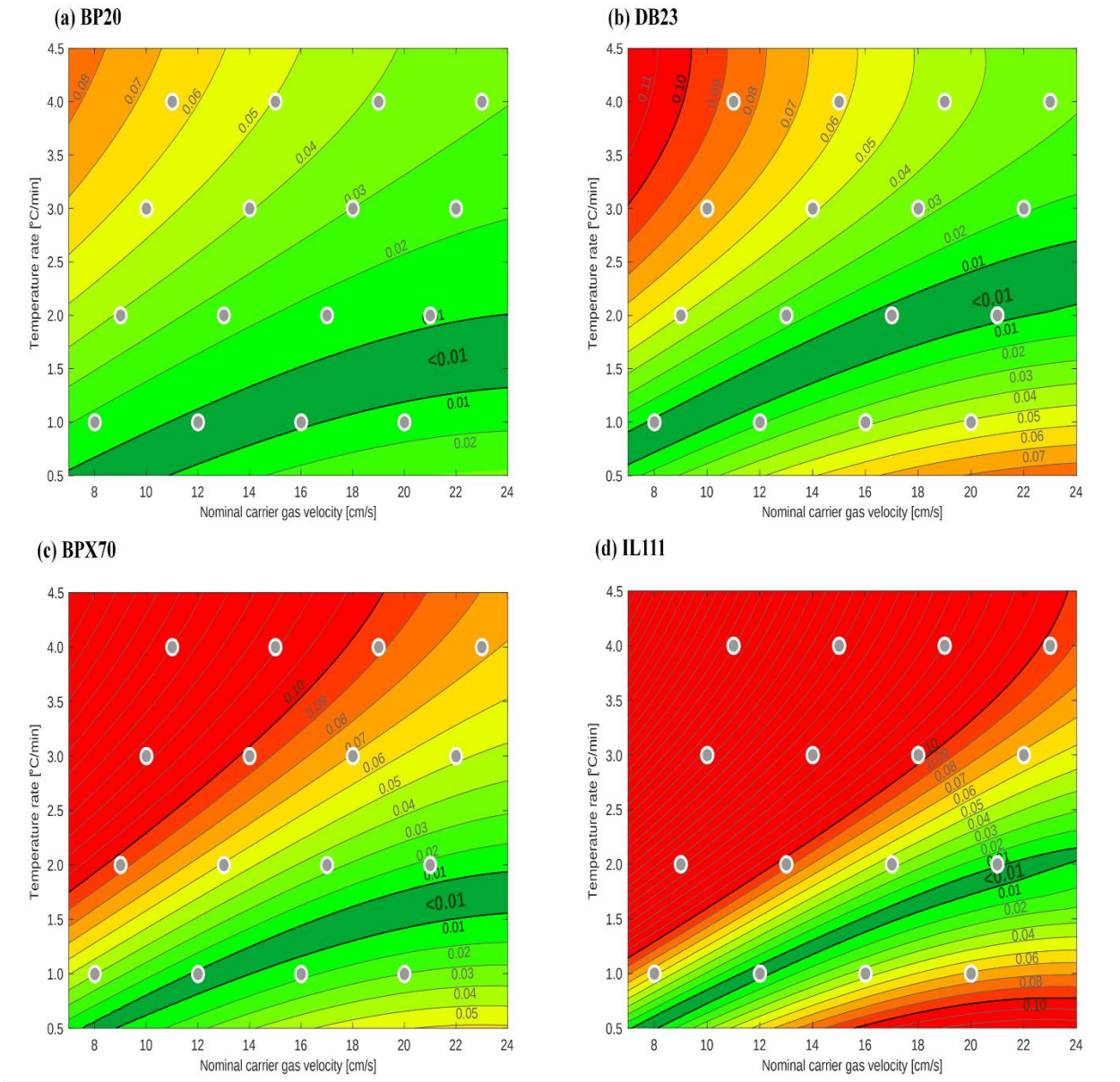


*Figure 12: Target surface plots showing the average deviation in ECL from the target values, on column: (a) BP20, (b) DB23, (c) BPX70 and (d) IL111, Nitrogen as carrier gas (Average deviation below 0.01 ECL units). Errors for the models are given in Appendix A3.*

## 4.2.5. Decisions on final conditions

A combined plot is created for all the column by combining the efficiency response surface plot (Figure 10) and selectivity response surface plots (Figure 12) of every column.

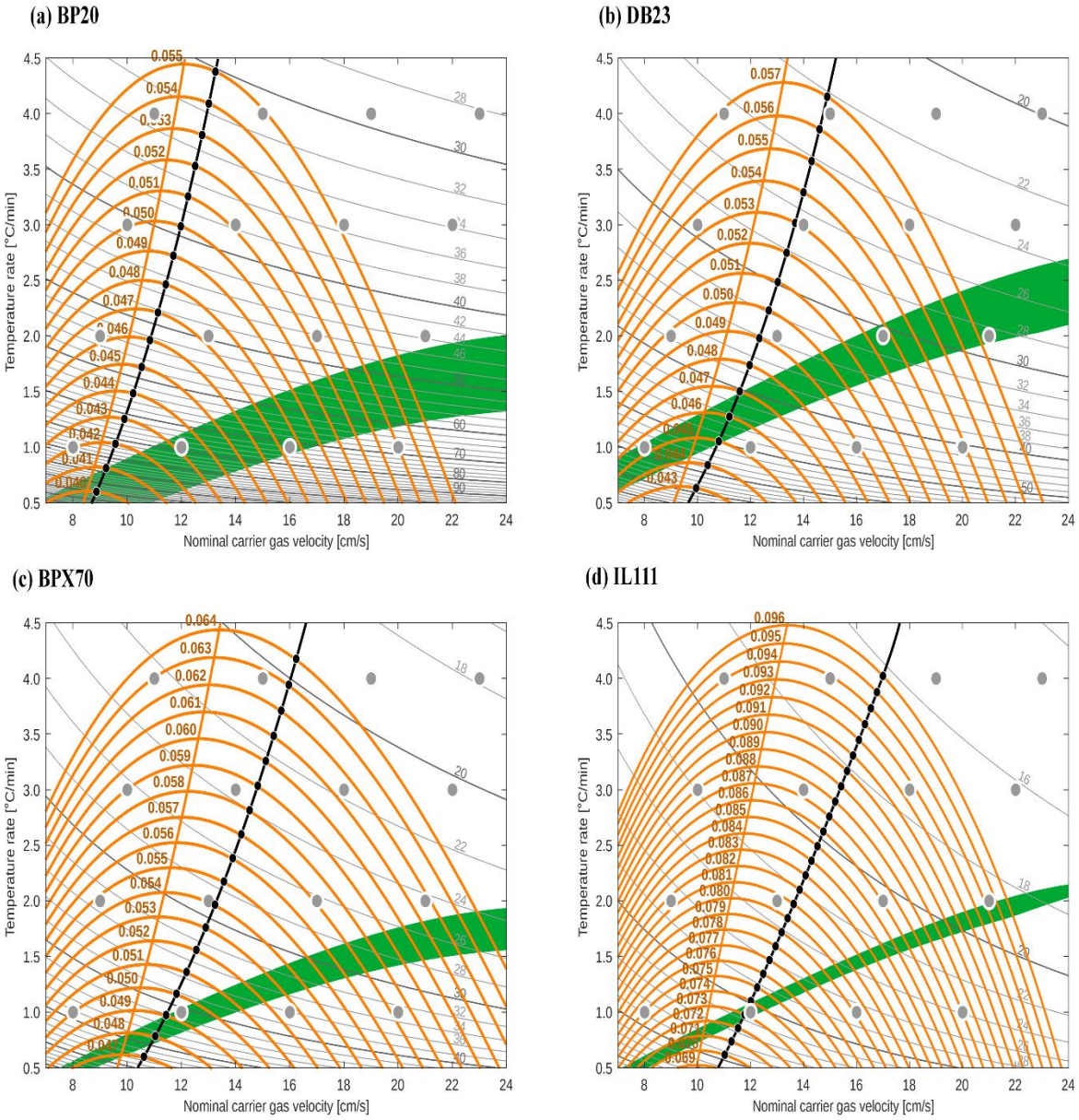


*Figure 13: Combined response surface plot of the selectivity and efficiency of the last eluting FAME (24.0), on column: (a) BP20, (b) DB23, (c) BPX70 and (d) IL111, Nitrogen as carrier gas (Average deviation below 0.01 ECL units).*

In Figure 13, the dark green areas are the same as in the selectivity plots. So, any condition in the dark green area near the black line will give best condition for the qualification with N2 gas.

A lot of compromises had to be made with selectivity and efficiency on every column except BP70 because either experimental condition did not fall on the desired zone or there was overlap in the

chromatogram on the desired experimental condition. As a result, different conditions were chosen which was column specific and they are given below-

- **BP20:** According to Fig. 13a, the optimal solution for BP20 (when the black line and green field intersect) is at very low flow rates. As shown in Figure 13a and explained elsewhere in the text, the elution temperature of the last compounds will be above the upper temperature limit when this column is applied with very low flow rates. To elute all compounds with nitrogen on this column it was therefore necessary to sacrifice some chromatographic efficiency by choosing a higher than optimal carrier gas velocity, or to choose a very low temperature rate and get a separation that takes long time. It was decided to not use rates lower than 1 $^{o}$C/min. The rate was therefore set to 1$^{o}$C/min and the velocity was set to 14 cm/s, which gives a condition suitable for reproducing the retention pattern (approximately in the middle of the green trace). So, the final condition was - the oven temperature was 60°C for 3 min, then 60°C/min to 160°C followed by the main temperature rate of 1.0°C/min to 260°C. Carrier gas velocity at injection was 14 cm/sec.
- **DB23:** DB23 column produces overlap between some components with D05 experimental condition. Keeping the same carrier gas velocity but increasing the temperate rate from 1.0°C/min to 1.3 0°C/min gives better separation according to the combined plots. That is why experimental condition modified as - oven temperature was 60°C for 3 min, then 60°C/min to 165°C followed by the main temperature rate of 1.3°C/min to 260°C. Carrier gas velocity at injection was 12 cm/sec.
- **BPX70 (30 m):** On BPX70 column, D05 was chosen as the final experimental condition. It is on the desired area on the combined plot, and it has given best chromatogram which was similar to the target. So, the final program was; oven temperature was 60°C for 3 min, then 60°C/min to 170°C followed by the main temperature rate of 1.0°C/min to 230°C. Carrier gas velocity at injection was 12 cm/sec. These conditions are therefore identical to one of the applied design points.
- **IL111:** In the case of IL111 column it is similar to BPX 70 column. Experimental condition of D05 has given the best chromatogram. So, the final condition selected as follows - oven temperature was 60°C for 3 min, then 6°C/min to 144°C followed by the main temperature rate of 1.0°C/min to 260°C. Carrier gas velocity at injection was 12 cm/sec. These conditions are therefore identical to one of the applied design points.

## 4.3. Comparison of He and $N_2$ methods

### 4.3.1. Selectivity

Figure 14 shows chromatograms on ECL scale of the original (helium) and the developed (nitrogen) programs. The retention patterns are highly similar. The largest deviation can be seen for the most unsaturated compounds on IL111. However, these deviate with less than a peak width from the target patterns acquired with helium.

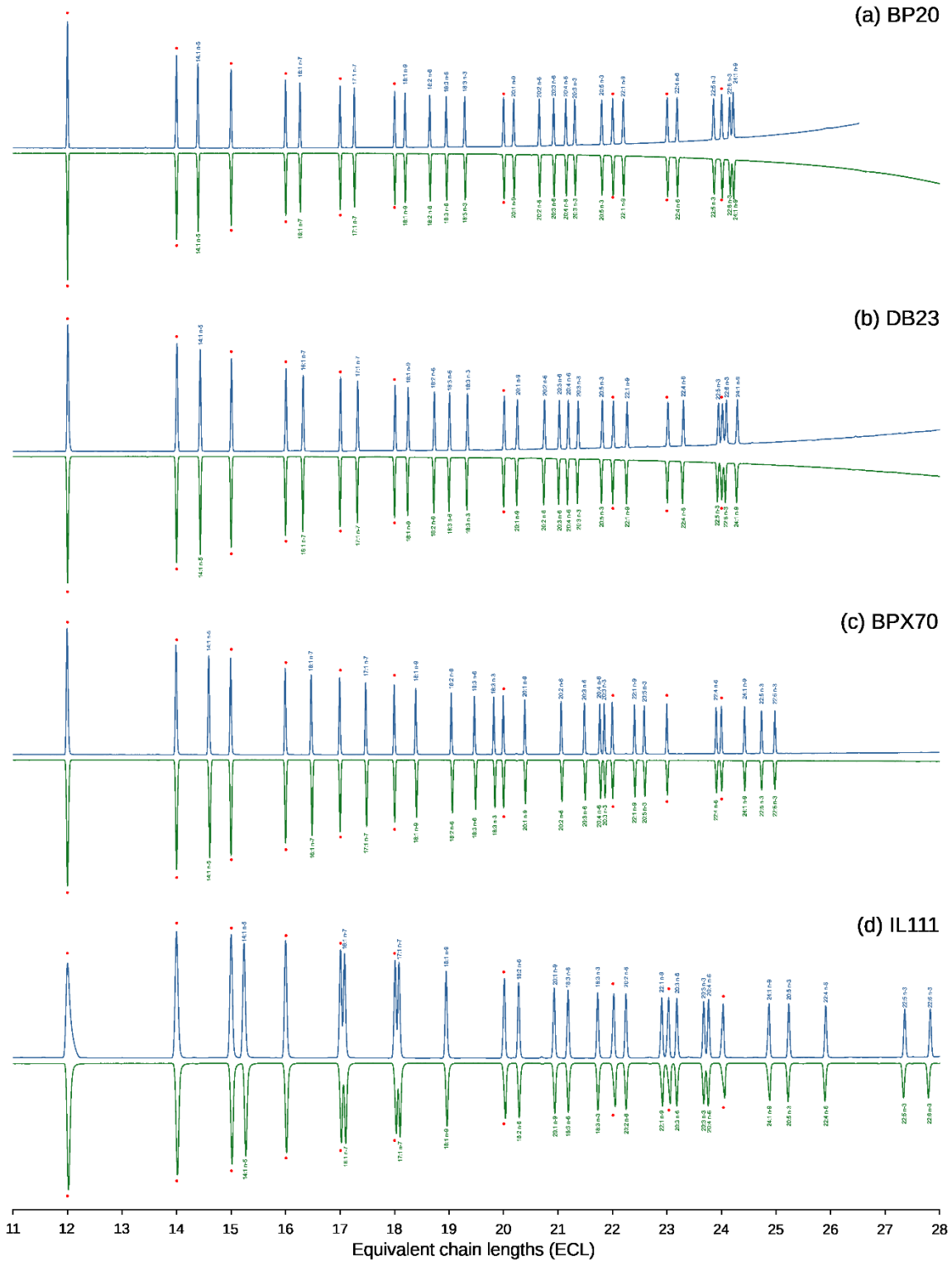


*Figure 14: Chromatograms on ECL scale displaying the retention patterns with helium (blue) and nitrogen (green) on BP20 (a), DB23 (b), BPX70 (c) and IL111 (d). Saturated compounds, which have their ECL value given by definition, are shown with red dots.*

## 4.3.2. Efficiency vs time

Changing from helium to nitrogen as carrier gas would usually mean that one gets lower chromatographic efficiency or that one has to accept that the analysis takes more time. Figure 15 shows the relationship between the efficiency (PPT) and the retention time of the last compound. A purely vertical transition in this plot means that the time is increased while the efficiency is maintained. A purely horizontal transition means that the efficiency is sacrificed while the analysis time is the same.

For BP20, DB23 and IL111 the transitions are close to vertical, meaning that the efficiency is approximately the same as before. An approximate doubling in retention times corresponds with the results presented in reference [17]. It should be emphasized that it is not possible to choose to sacrifice resolution instead of time and still be able to reproduce the retention pattern. Shorter retention times can be achieved by increasing the temperature ramp rate, but then the conditions will not match the green traces in Figure 13.

BPX70 shows an almost horizontal transition. Contrary to the case for the other columns, for BPX70 it is not only a change in carrier gas, but also a reduction in column length. These results indicate that if one wants to change carrier gas from helium to nitrogen, one should also reduce the column length if one requires a method that can be done within the same time as before.

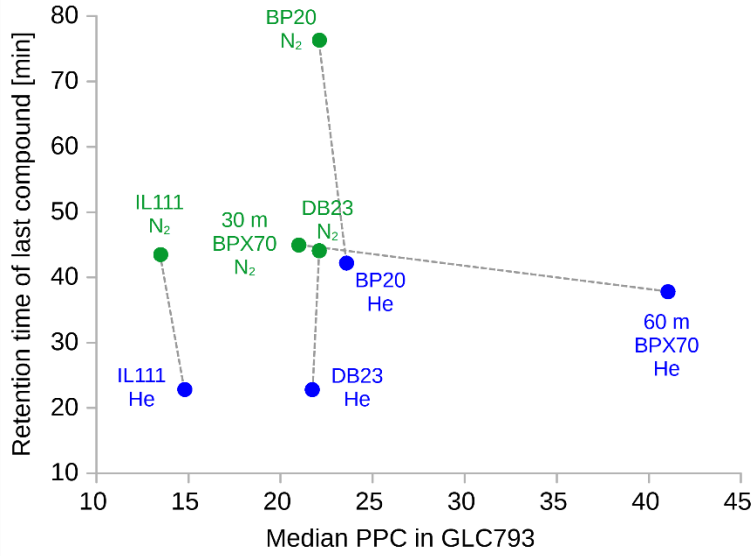


*Figure 15: The relationship between average PPC and the retention time for the last compound for the programs with helium (blue) and nitrogen (green) as carrier gas.*

## 4.3.3. Elution temperatures

The last eluting compound was different in different columns. For BP20 and DB23 column the last eluting compound was 24:1 n-9 where in BPX70 and IL111 columns the last eluting compound was 22:4 n-6. This elution pattern was the same with both He and $N_2$ gas. Figure 16 shows the elution temperature of the last eluting compound in GLC793 sample in different column with he and N2 gas.

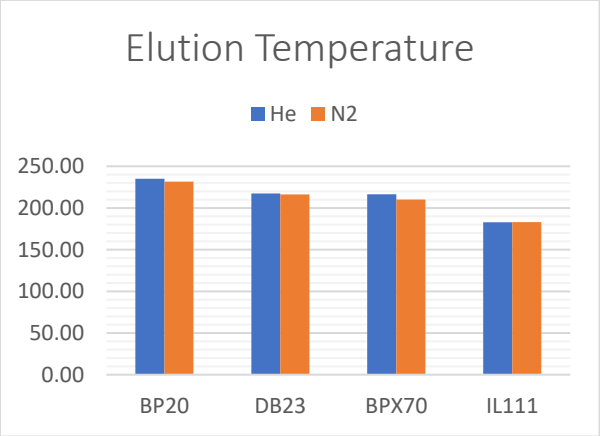


*Figure 16: Elution Temperature of last compound in different column with He and $N_2$ carrier gas.*

In the experiments with $N_2$, application of a lower temperature rate (and a shorter column in the case of BPX70) resulted in a lower elution temperature of the last eluting compound. From Figure 14, it can be seen that elution temperature of the last eluting compound is slightly lower with N2 compared to He in all the column except IL111.

In IL111column the elution temperature of 22:6 n-3 with N2 is 183.11 $^0$C which is slightly higher than with He which is 182.80 $^0$C. Increased oven temperature generally reduces the retention time of the compound. In Column with He gas the retention times are much lower compared to retention times with N2, except IL111 column. Although in IL111 column the temperature with He was slightly lower than N2 the retention time was also lower.

## 4.3.4. Comparison of quantitative results

The percentage of fatty acids were calculated for EPA (20:5 n-3), DPA (22:5 n-3) and DHA (22:6 n-3) in all the samples. Then correlations among all the columns for EPA, DPA and DHA were measured as $R^2$ values for evaluation of columns.

BP20 column gives the best correlations for all three fatty acids. From Figure 17, it can be seen that, in case of EPA, correlation between He and N2 in BP20 column is same ($R^2$=0.999). $R^2$ value is slightly lower (0.988) in case of correlation between He and N2 in for DHA.

DB23 column gives the lowest $R^2$ values among all the columns for correlation between helium and nitrogen. For EPA, DPA the $R^2$ values are 0.689, 0.573 which indicates a very poor correlation between He and N2. For DHA the $R^2$ value is 0.872 which illustrates better correlation between the gases than EPA and DPA.

In case of the BPX70 column, the $R^2$ for the two-carrier gas were 0.973, 0.974 and 0.916 consecutively for EPA, DPA and DHA. This column gives the second-best correlation between the He and $N_2$ gas.

In the case of the IL111 column, the $R^2$ for the two-carrier gas was 0.826 for EPA. In the case of DPA and DHA correlation values are 0.7181 and 0.713 consecutively which are lower than EPA. This also depicts a poor correlation between helium and nitrogen.

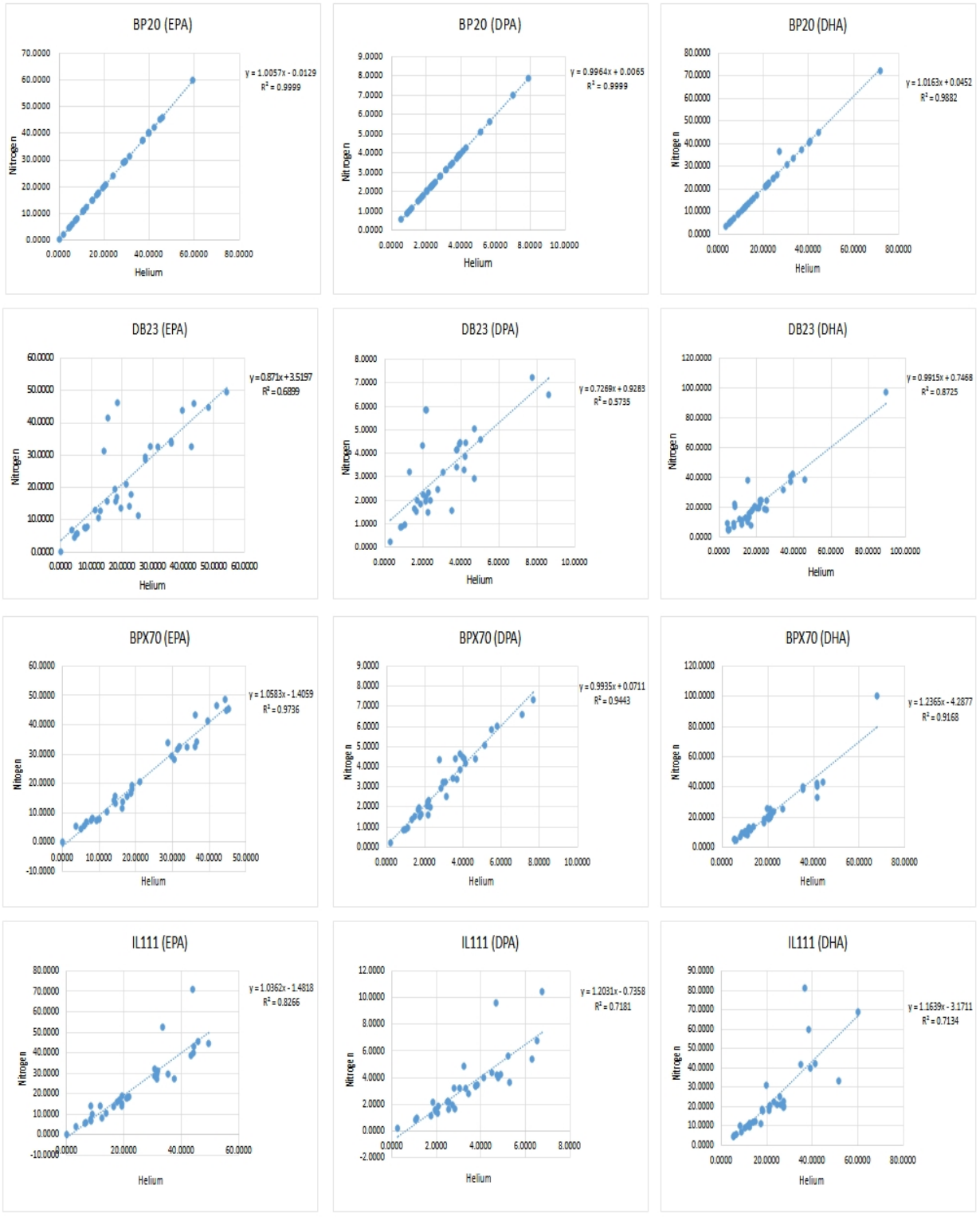


*Figure 17: Correlation plots for EPA, DPA and DHA quantified in omega-3 supplements with the two different carrier gases.*

### 4.3.5. Comparison of precision

Precision study was conducted in all the four columns to check the preciseness of the analytical procedure. First, fatty acids EPA (20:5 n-3), DPA (22:5 n-3) and DHA (22:6 n-3) were calculated for mg/mg of FA. Then relative standard deviation was measured to show precision. All the nitrogen programs have relative standard deviation below 1%, which indicates that all the columns have produced precise results. BPX70 column has lowest RSD (0.13%) for DHA where BP20 highest RSD (0.73%).

Precision study was also conducted in all the four columns with He. With He, maximum RSD is 0.99% for EPA in DB23 column and all the columns have RSD below 1%. This indicates that all the columns have produced precise results with He also. Figure 18 illustrates the difference between RSD values for EPA, DPA and DHA among all the columns with He and N2 as carrier gas. From Figure 18, it can be seen that there is no specific pattern of difference in RSD values with He and N2. The only conclusion is that analytical procedure is precise with both gases.

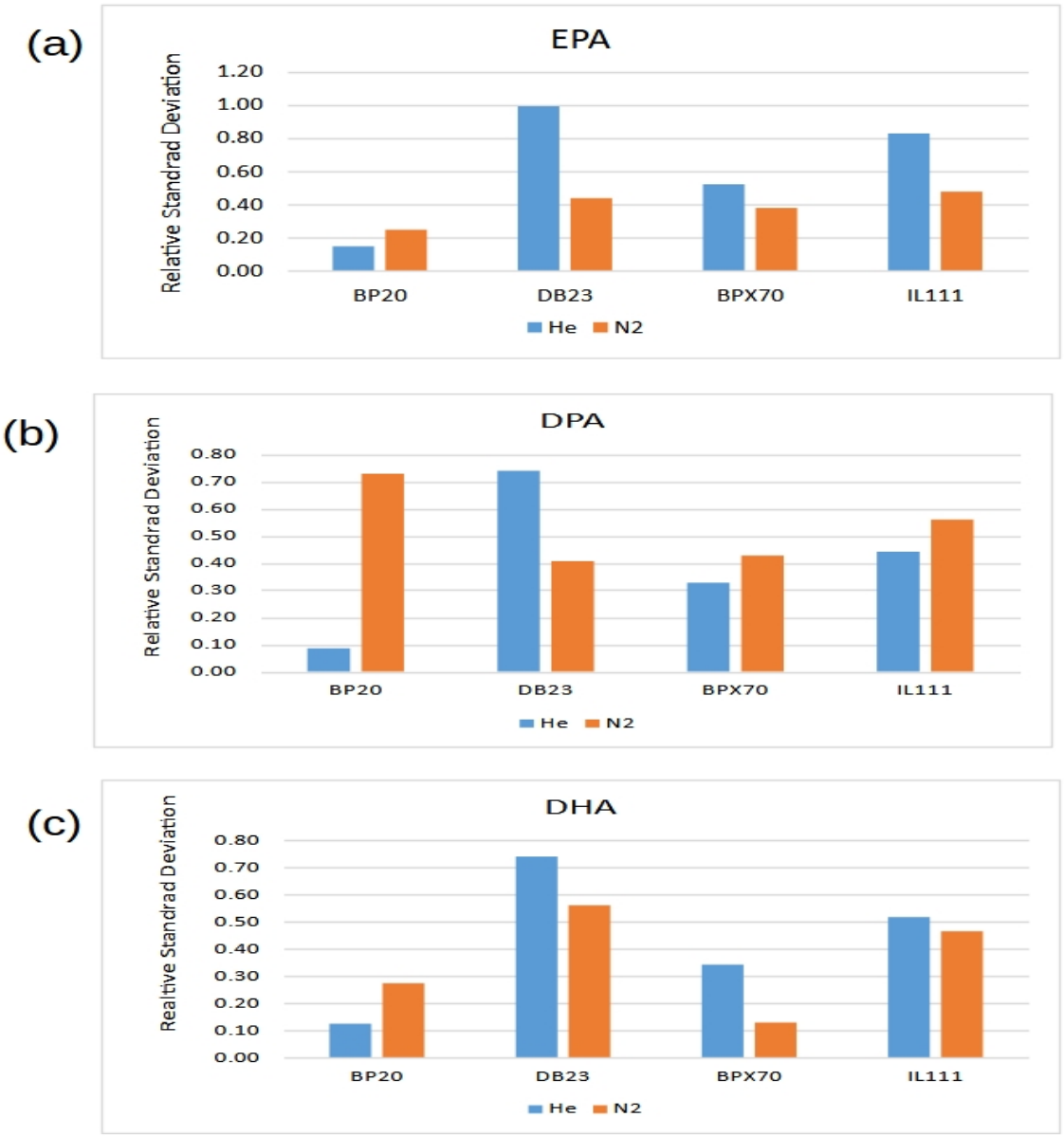


*Figure 18: Precision of analyses of EPA (a), DPA (b) and DHA (c) in all columns with He and Nitrogen as a carrier gas.*

# 5. Conclusions and further work

## 5.1 Conclusions

- Column bleed is higher in medium polar columns. In the study, medium polar column DB23 had 73% column bleed and BP20 had 31% column bleed.
- Shifts of ECL values for 20:5 n-3 observed to increase with increased polarity of the columns.
- Column efficiency is found to decrease in FAME analysis with increasing column polarity.
- Critical overlaps were also found to increase with increased polarity. Very highly polar column IL111 had most overlaps.
- Medium polar column BP20 and high polar column BPX70 provided better quantitative results compared to other columns.
- Retention time of quantitative FAME analysis is found to increase in nitrogen compared to helium.

  Precision of the analytical procedure was maximum 1% with both He and N2 which concludes the preciseness of the analysis.

## 5.2 Recommendations for further work

- In very highly polar column IL111, column bleed was lowest and at that point there was almost no background. So, it is not necessary to run IL111 at conditions where the bleed is significant.
- Method transfer from helium to nitrogen gas was found best in BP20 column and BPX70 which has medium and high polarity consecutively. This does not go along with the reasoning of polarity for decreasing efficiency. Further study needs to be done for polarity study of the columns.

# References


1. Chhaganlal M, Skartland LK, Mjøs SA. Transfer of retention patterns in gas chromatography by means of response surface methodology. Journal of Chromatography A. 2014 Mar 7;1332:64-72.
2. Eriksson L, Johansson E, Kettaneh-Wold N, Wikström C, Wold S. Design of Experiments-principles and Applications: Umetrics AB. Umeå, Sweden. 2008.
3. Bezerra MA, Santelli RE, Oliveira EP, Villar LS, Escaleira LA. Response surface methodology (RSM) as a tool for optimization in analytical chemistry. Talanta. 2008 Sep 15;76(5):965-77.
4. Lin CC, Wasta Z, Mjøs SA. Evaluation of the retention pattern on ionic liquid columns for gas chromatographic analyses of fatty acid methyl esters. Journal of Chromatography A. 2014 Jul 11;1350:83-91.
5. Ferreira SL, Bruns RE, da Silva EG, Dos Santos WN, Quintella CM, David JM, de Andrade JB, Breitkreitz MC, Jardim IC, Neto BB. Statistical designs and response surface techniques for the optimization of chromatographic systems. Journal of chromatography A. 2007 Jul 27;1158(1-2):2-14.
6. Myers RH, Montgomery DC, Anderson-Cook CM. Response surface methodology: process and product optimization using designed experiments. John Wiley & Sons; 2016 Jan 4.
7. Ferreira SC, Bruns RE, Ferreira HS, Matos GD, David JM, Brandão GC, da Silva EP, Portugal LA, Dos Reis PS, Souza AS, Dos Santos WN. Box-Behnken design: An alternative for the optimization of analytical methods. Analytica chimica acta. 2007 Aug 10;597(2):179-86.
8. Brereton RG. Chemometrics: data analysis for the laboratory and chemical plant. John Wiley & Sons; 2003 Jul 25
9. Skartland LK, Mjøs SA, Grung B. Experimental designs for modeling retention patterns and separation efficiency in analysis of fatty acid methyl esters by gas chromatography–mass spectrometry. Journal of Chromatography A. 2011 Sep 23;1218(38):6823-31.
10. C. Graham, Analytical instrumentation performance characterstics and quality, Bristol: John wiley and sons LTD, 2000.

11. Seppänen-Laakso T, Laakso I, Hiltunen R. Analysis of fatty acids by gas chromatography, and its relevance to research on health and nutrition. Analytica Chimica Acta. 2002 Aug 16;465(1-2):39-62.
12. Martin AJ, Synge RL. A new form of chromatogram employing two liquid phases: A theory of chromatography. 2. Application to the micro-determination of the higher monoamino-acids in proteins. Biochemical Journal. 1941 Dec;35(12):1358.
13. James AT, Martin AJ. Gas-liquid partition chromatography: the separation and micro-estimation of volatile fatty acids from formic acid to dodecanoic acid. Biochemical Journal. 1952 Mar;50(5):679.
14. Eder K. Gas chromatographic analysis of fatty acid methyl esters. Journal of Chromatography B: Biomedical Sciences and Applications. 1995 Sep 15;671(1-2):113-31.
15. Sciotto C, Mjøs SA. Trans isomers of EPA and DHA in omega-3 products on the European market. Lipids. 2012 Jul;47:659-67.
16. Christie WW. Gas chromatography and lipids: a practical guide. (No Title). 1989 Dec.
17. Waktola HD, Mjøs SA. Chromatographic efficiency of polar capillary columns applied for the analysis of fatty acid methyl esters by gas chromatography. Journal of separation science. 2018 Apr;41(7):1582-92.
18. Meier S, Mjøs SA, Joensen H, Grahl-Nielsen O. Validation of a one-step extraction/methylation method for determination of fatty acids and cholesterol in marine tissues. Journal of Chromatography A. 2006 Feb 3;1104(1-2):291-8.
19. Wittkowski R., Matissek R.; Capillary Gas Chromatography in Food Control and Research. 1993: by Technomic publishing company Inc. Lancaster, Pennsylvania, USA. p. 19-33. 11.
20. Fowlis I. A.; Gas Chromatography. 1995: by John Wiley & Sons Ltd. 2nd ed. University of Greenwich, Uk. p. 1- 100. 12.
21. Harvey D.; Modern analytical chemistry. 2000: by The McGraw-Hill Companies, Inc., United States of America. p. 547-56
22. Blumberg LM. Plate height formula widely accepted in GC is not correct. Journal of chromatography. A. 2011 Dec 2;1218(48):8722-3.

23. Usher KM, Simmons CR, Dorsey JG. Modeling chromatographic dispersion: A comparison of popular equations. Journal of Chromatography A. 2008 Jul 25;1200(2):122-8.
24. Blumberg LM. Theory of fast capillary gas chromatography–Part 3: Column performance vs. gas flow rate. Journal of High Resolution Chromatography. 1999 Jul 1;22(7):403-13.
25. Kovats VE. Gas-chromatographische charakterisierung organischer verbindungen. Teil 1: retentionsindices aliphatischer halogenide, alkohole, aldehyde und ketone. Helvetica Chimica Acta. 1958;41(7):1915-32.
26. Ettre LS. The retention index system; Its utilization for substance identification and liquid phase characterization. Chromatographia. 1973 Nov;6(11):489-95.
27. Ettre L.S.; Retention Index Expressions.; Chromatographia, 2003. 58 (7-8): p.491- 494. 20.
28. Castello G. Retention index systems: alternatives to the n-alkanes as calibration standards. Journal of Chromatography A. 1999 May 21;842(1-2):51-64.
29. Woodford FP, Van Gent CM. Gas-liquid chromatography of fatty acid methyl esters: the" carbon-number" as a parameter for comparison of columns. Journal of Lipid Research. 1960;1:188-90.
30. Van Den Dool H., Kratz P.D.; A generalization of the retention index system including linear temperature programmed gas-liquid partition chromatography. J. Chvomalog., 1963. 11: p. 463-471. 23.
31. Wasta Z, Mjøs SA. A database of chromatographic properties and mass spectra of fatty acid methyl esters from omega-3 products. Journal of Chromatography A. 2013 Jul 19;1299:94-102.
32. Mjøs SA. Prediction of equivalent chain lengths from two-dimensional fatty acid retention indices. Journal of Chromatography A. 2006 Jul 28;1122(1-2):249-54.
33. Ettre LS. Separation values and their utilization in column characterization: Part II: Possible improvement in the use of the separation values to express relative column performance. Chromatographia. 1975 Jul;8(7):355-7.
34. M. Czernicka, M. Kowalska, "Determination of Fatty Acids in Food Samples by Gas Chromatography Techniques," Molecules 2019, 24(10), 1987.
35. J. Huang, L. Li, Y. Wang, "Comparison of Selectivity of Cyanopropyl and PEG Columns in Fatty Acid Analysis," J. Sep. Sci. 2018, 41(8), 1814-1822.

36. M. Tobiszewski, J. Namiesnik, "Ionic Liquids in Gas Chromatography," Crit. Rev. Anal. Chem. 2011, 41(3), 196-205
37. Mjøs SA, Waktola HD. Optimizing the relationship between chromatographic efficiency and retention times in temperature-programmed gas chromatography. Journal of separation Science. 2015 Sep;38(17):3014-27.
38. Desalegn SK. *Gas Chromatography optimization using experimental design and surface response methodology* (Master's thesis, The University of Bergen).

# Appendix

## A1. Errors for the retention time models of the last compound

### A1.1 Plots of predicted vs measured

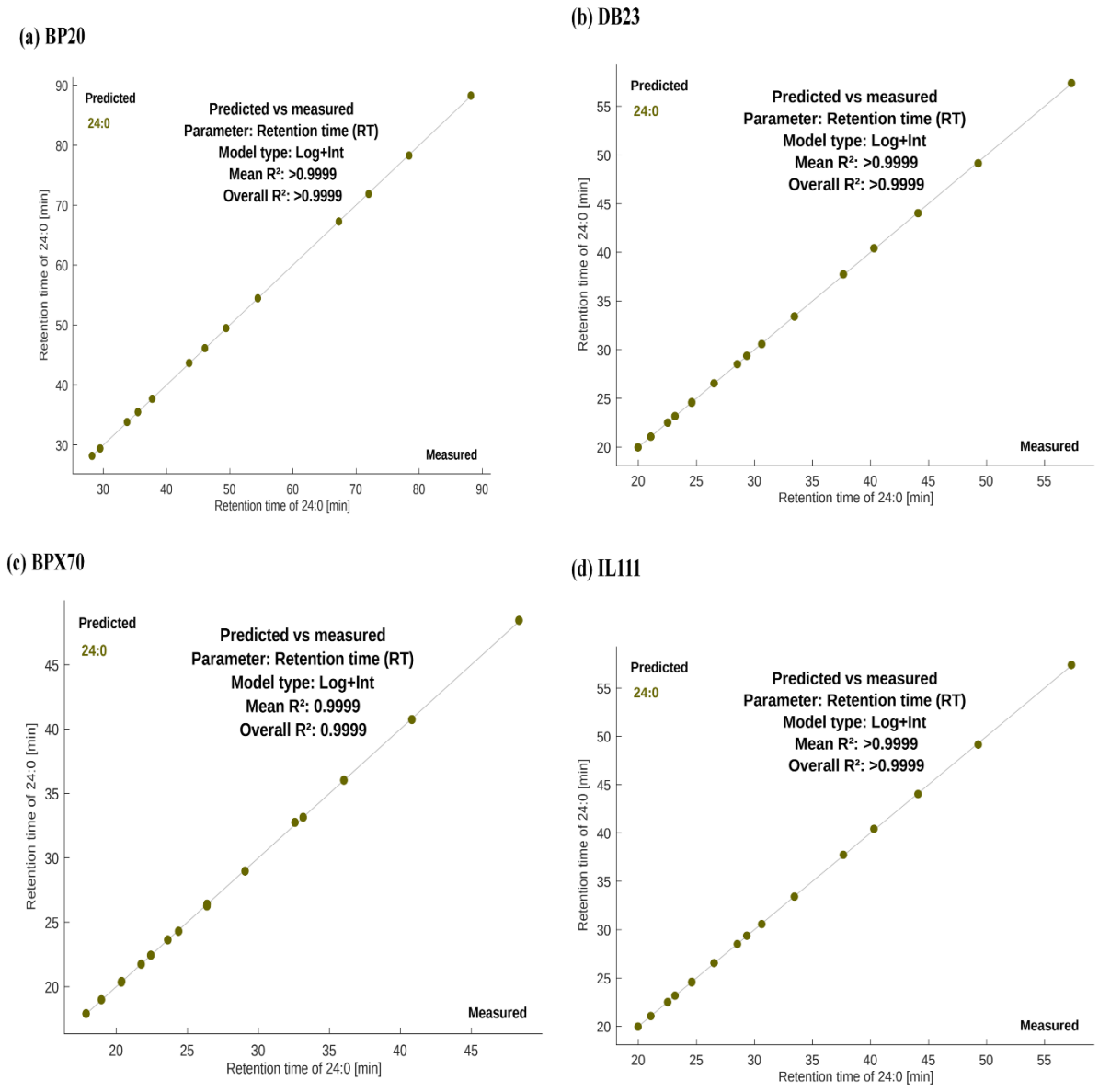


*Fig A 1:Predicted vs measured values for retention time models of 24:0*

## A1.2. Error in BP20 column for Retention time of 24:0.

```
PREDICTED VS MEASURED:
Model type: Log+Int
Parameter: Retention time (RT)
      R²        Bias     RMSE     RMSE(adj)  N. Exp.
-----------------------------------------------------
24:0  >0.9999   -0.0017  0.07469  0.08977    13     (3,4,8)*
-----------------------------------------------------
*These programs have been excluded from the model, either because the peak did not elute, or also
because of overlap in the case of EFF models.
```

## A1.3. Error in DB23 column for Retention time 0f 24:0.

```
PREDICTED VS MEASURED:
Model type: Log+Int
Parameter: Retention time (RT)
      R²        Bias        RMSE     RMSE(adj)  N. Exp.
-----------------------------------------------------------
24:0  >0.9999   -9.204e-05  0.06113  0.07059    16
-----------------------------------------------------------
```

## A1.4. Error in BPX70 column for Retention time of 24:0.

```
PREDICTED VS MEASURED:
Model type: Log+Int
Parameter: Retention time (RT)
      R²      Bias       RMSE     RMSE(adj)  N. Exp.
-------------------------------------------------------
24:0  0.9999  0.0009077  0.06959  0.08036    16
-------------------------------------------------------
```

## A1.5. Error in IL111 column for Retention time of 24:0.

```
PREDICTED VS MEASURED:
Model type: Log+Int
Parameter: Retention time (RT)
      R²      Bias       RMSE    RMSE(adj)  N. Exp.
-------------------------------------------------------
24:0  0.9999  0.0007767  0.0694  0.08014    16
-------------------------------------------------------
```

# A2. Errors for the peak width models

## A2.1 Plots of predicted vs measured

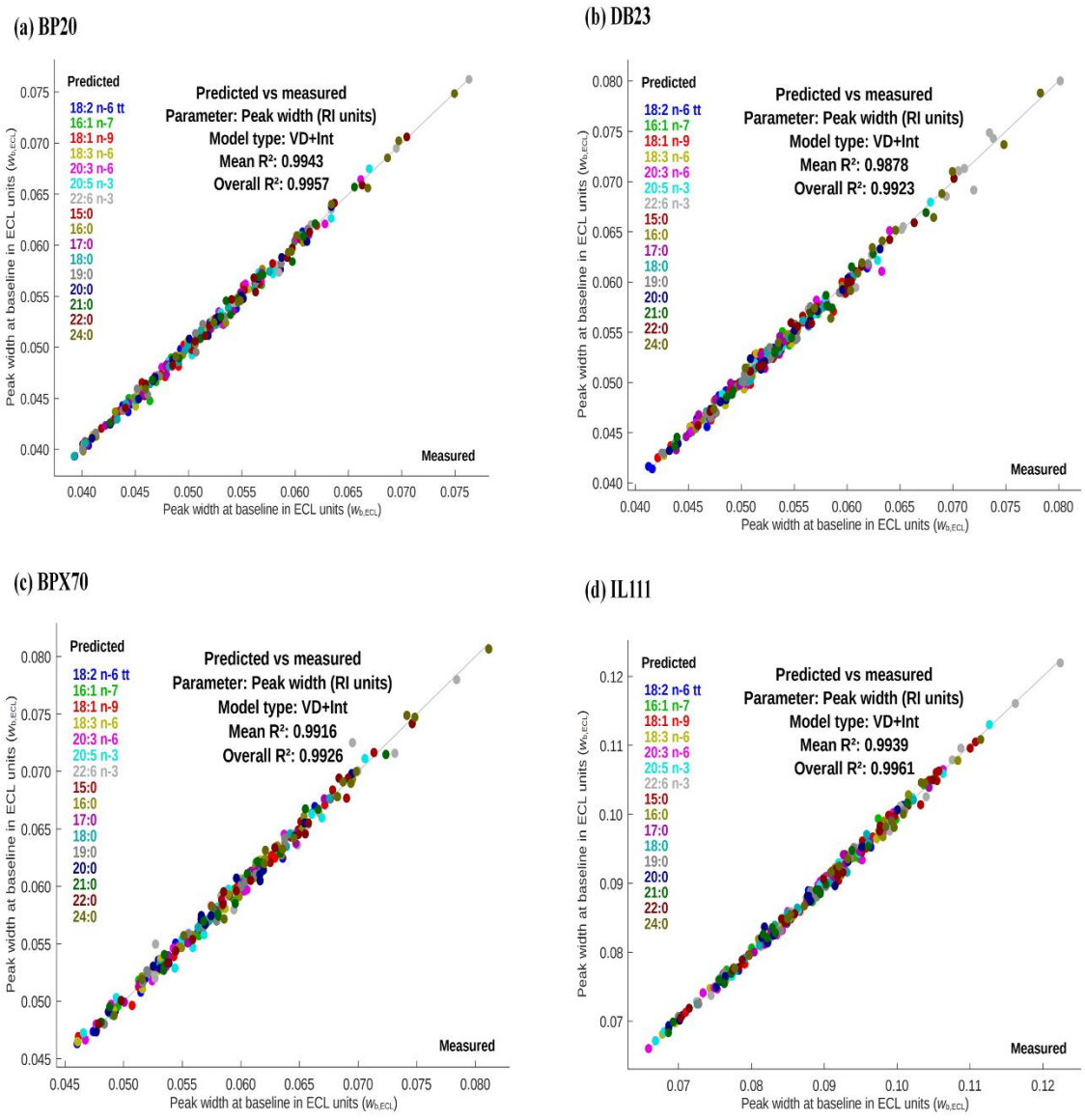


*Fig A 2: Predicted vs measured values for peak width is ECL units*

# A2.2. Error in BP20 column for Peak widths in ECL units.

PREDICTED VS MEASURED:

Model type: VD+Int

Parameter: Peak width (RI units)

| | $R^2$ | Bias | RMSE | RMSE(adj) | N. Exp. | |
|---|---|---|---|---|---|---|
| 18:2 n-6 tt | 0.9923 | 5.089e-18 | 0.0005274 | 0.0006809 | 15 | (3) |
| 16:1 n-7 | 0.9908 | 1.214e-17 | 0.0005539 | 0.0007006 | 16 | |
| 18:1 n-9 | 0.9931 | 8.327e-18 | 0.0004964 | 0.0006408 | 15 | (6) |
| 18:3 n-6 | 0.9936 | 8.674e-19 | 0.0004406 | 0.0005573 | 16 | |
| 20:3 n-6 | 0.9936 | -5.638e-18 | 0.0005069 | 0.0006412 | 16 | |
| 20:5 n-3 | 0.9929 | -1.735e-18 | 0.0005549 | 0.0007848 | 12 | (2,4,7,12) |
| 22:6 n-3 | 0.997 | -9.252e-18 | 0.0004454 | 0.0007715 | 9 | (2,3,4,5,7,8,12) |
| 15:0 | 0.9937 | 2.602e-18 | 0.0004092 | 0.0005176 | 16 | |
| 16:0 | 0.9938 | -7.373e-18 | 0.0004411 | 0.0005579 | 16 | |
| 17:0 | 0.9968 | -4.337e-18 | 0.0003325 | 0.0004206 | 16 | |
| 18:0 | 0.9975 | 7.373e-18 | 0.0002929 | 0.0003705 | 16 | |
| 19:0 | 0.991 | 2.168e-18 | 0.0005506 | 0.0006965 | 16 | |
| 20:0 | 0.9962 | -1.171e-17 | 0.0003839 | 0.0004856 | 16 | |
| 21:0 | 0.9927 | -4.626e-18 | 0.0005084 | 0.0006564 | 15 | (5) |
| 22:0 | 0.9965 | -5.551e-18 | 0.0004279 | 0.0005525 | 15 | (4) |
| Mean | 0.9941 | -7.768e-19 | 0.0004581 | 0.0006023 | 15 | |

* These programs have been excluded from the model, either because the peak did not elute, or also because of overlap in the case of EFF models.

# A2.3. Error in DB23 column for peak widths in ECL units.

PREDICTED VS MEASURED:

Model type: VD+Int

Parameter: Peak width (RI units)

| | $R^2$ | Bias | RMSE | RMSE(adj) | N. Exp. |
|---|---|---|---|---|---|
| 18:2 n-6 tt | 0.9879 | -6.939e-18 | 0.0005925 | 0.0007494 | 16 |
| 16:1 n-7 | 0.9874 | -3.469e-18 | 0.0004706 | 0.0005952 | 16 |
| 18:1 n-9 | 0.9741 | 4.337e-19 | 0.0007747 | 0.0009799 | 16 |
| 18:3 n-6 | 0.9864 | 4.77e-18 | 0.0005519 | 0.0006981 | 16 |
| 20:3 n-6 | 0.9832 | 5.204e-18 | 0.0007241 | 0.0009159 | 16 |
| 20:5 n-3 | 0.9936 | -2.602e-18 | 0.0004518 | 0.0005714 | 16 |
| 22:6 n-3 | 0.9839 | -6.939e-18 | 0.0009972 | 0.001261 | 16 |
| 14:0 | 0.9577 | -4.77e-18 | 0.0006068 | 0.0007675 | 16 |
| 15:0 | 0.9855 | -6.072e-18 | 0.0004327 | 0.0005473 | 16 |
| 16:0 | 0.9943 | 4.337e-19 | 0.0002825 | 0.0003573 | 16 |
| 17:0 | 0.9796 | 8.674e-19 | 0.0006571 | 0.0008312 | 16 |
| 18:0 | 0.995 | -1.301e-18 | 0.0003231 | 0.0004087 | 16 |
| 19:0 | 0.9878 | 6.505e-18 | 0.0005903 | 0.0007467 | 16 |
| 20:0 | 0.9934 | 2.168e-18 | 0.0004561 | 0.000577 | 16 |
| 21:0 | 0.993 | -1.171e-17 | 0.0005267 | 0.0006662 | 16 |
| 22:0 | 0.995 | -4.337e-18 | 0.0004601 | 0.000582 | 16 |
| 24:0 | 0.9853 | 0 | 0.0009794 | 0.001239 | 16 |
| Mean | 0.9861 | -1.633e-18 | 0.000581 | 0.000735 | 16 |

# A2.4. Error in BPX70 column for peak widths in ECL units.

PREDICTED VS MEASURED:
Model type: VD+Int
Parameter: Peak width (RI units)

| | $R^2$ | Bias | RMSE | RMSE(adj) | N. Exp. |
|---|---|---|---|---|---|
| 18:2 n-6 tt | 0.9937 | 3.903e-18 | 0.000444 | 0.0005616 | 16 |
| 16:1 n-7 | 0.9908 | -7.373e-18 | 0.000433 | 0.0005477 | 16 |
| 18:1 n-9 | 0.9934 | 8.674e-19 | 0.0004436 | 0.0005611 | 16 |
| 18:3 n-6 | 0.995 | 0 | 0.0003845 | 0.0004863 | 16 |
| 20:3 n-6 | 0.9936 | -7.806e-18 | 0.0004989 | 0.0006311 | 16 |
| 20:5 n-3 | 0.9877 | -5.204e-18 | 0.0007335 | 0.0009279 | 16 |
| 22:6 n-3 | 0.9743 | 9.541e-18 | 0.001182 | 0.001496 | 16 |
| 15:0 | 0.9889 | 7.806e-18 | 0.0004571 | 0.0005781 | 16 |
| 16:0 | 0.9914 | 1.214e-17 | 0.0004187 | 0.0005296 | 16 |
| 17:0 | 0.9953 | -5.638e-18 | 0.0003292 | 0.0004164 | 16 |
| 18:0 | 0.9975 | 8.674e-19 | 0.0002609 | 0.00033 | 16 |
| 19:0 | 0.995 | 0 | 0.000398 | 0.0005034 | 16 |
| 20:0 | 0.9904 | -8.24e-18 | 0.000571 | 0.0007223 | 16 |
| 21:0 | 0.9894 | -5.204e-18 | 0.0006489 | 0.0008208 | 16 |
| 22:0 | 0.9946 | 1.301e-18 | 0.000518 | 0.0006552 | 16 |
| 24:0 | 0.9951 | 2.602e-18 | 0.0005925 | 0.0007495 | 16 |
| Mean | 0.9916 | -2.711e-20 | 0.0005196 | 0.0006573 | 16 |

# A2.5. Error in IL111 column for peak widths in ECL units.

PREDICTED VS MEASURED:

Model type: VD+Int

Parameter: Peak width (RI units)

| | $R^2$ | Bias | RMSE | RMSE(adj) | N. Exp. |
|---|---|---|---|---|---|
| 18:2 n-6 tt | 0.9954 | -2.602e-18 | 0.0006085 | 0.0007697 | 16 |
| 16:1 n-7 | 0.9898 | -1.128e-17 | 0.0007614 | 0.0009631 | 16 |
| 18:1 n-9 | 0.9962 | -8.674e-19 | 0.0005215 | 0.0006597 | 16 |
| 18:3 n-6 | 0.9979 | -3.469e-18 | 0.0004598 | 0.0005817 | 16 |
| 20:3 n-6 | 0.9951 | 2.602e-18 | 0.0007942 | 0.001005 | 16 |
| 20:5 n-3 | 0.9985 | 8.674e-19 | 0.0004869 | 0.0006158 | 16 |
| 22:6 n-3 | 0.9973 | -1.214e-17 | 0.0007272 | 0.0009198 | 16 |
| 15:0 | 0.9822 | -1.475e-17 | 0.0008619 | 0.00109 | 16 |
| 16:0 | 0.989 | -9.541e-18 | 0.0007261 | 0.0009184 | 16 |
| 17:0 | 0.9944 | -4.337e-18 | 0.0005508 | 0.0006967 | 16 |
| 18:0 | 0.9942 | -1.735e-17 | 0.0006112 | 0.0007732 | 16 |
| 19:0 | 0.9933 | 0 | 0.0006661 | 0.0008425 | 16 |
| 20:0 | 0.992 | 6.072e-18 | 0.0007802 | 0.0009869 | 16 |
| 21:0 | 0.9957 | -7.806e-18 | 0.0005923 | 0.0007492 | 16 |
| 22:0 | 0.9971 | -6.072e-18 | 0.000505 | 0.0006387 | 16 |
| 24:0 | 0.9946 | 6.072e-18 | 0.0006665 | 0.000843 | 16 |
| Mean | 0.9939 | -4.662e-18 | 0.000645 | 0.0008158 | 16 |

# A3. Errors for the selectivity (ECL) models

## A3.1 Plots of predicted vs measured

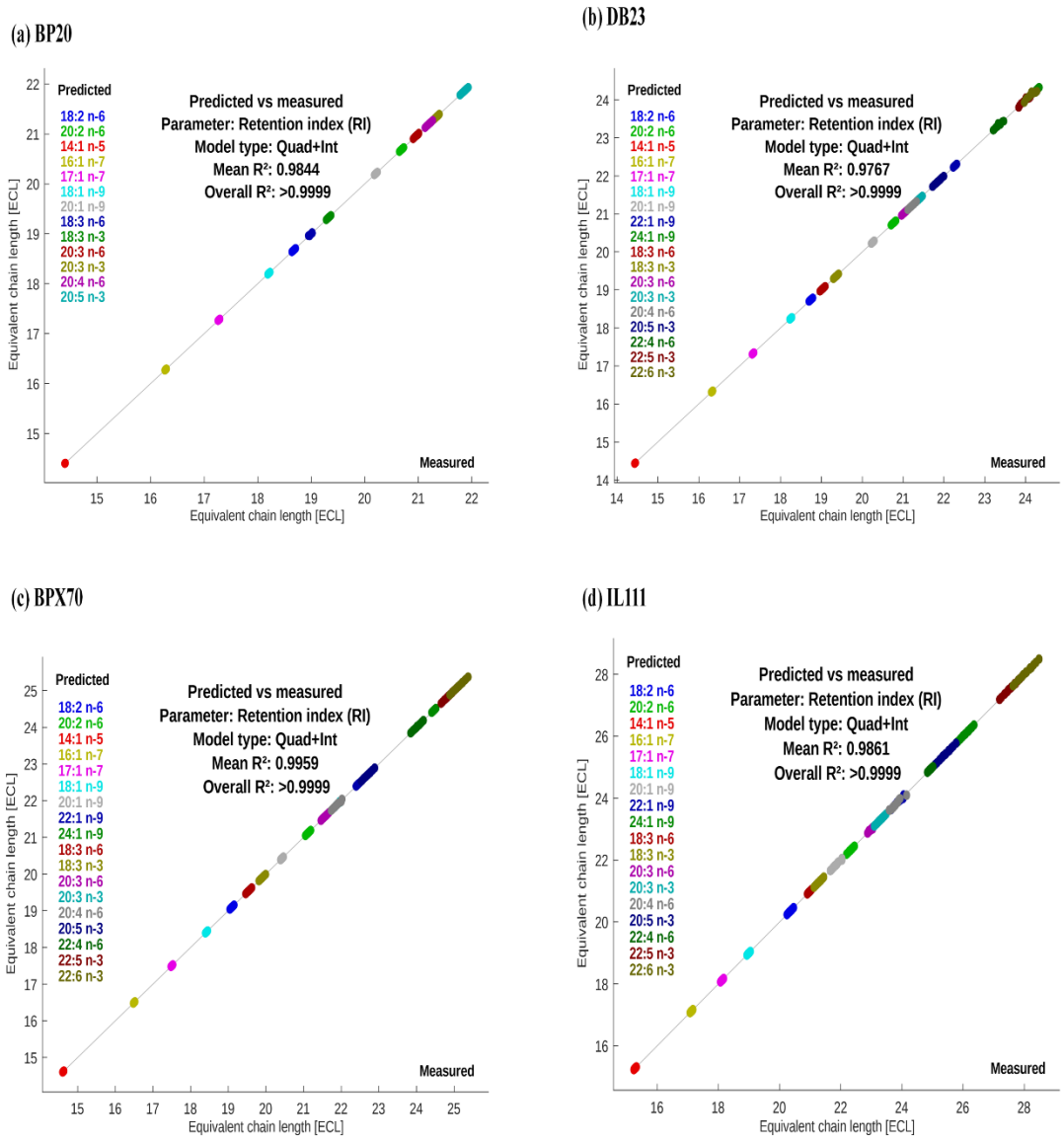


*Fig A 3: Predicted vs measured values for selectivity models*

# A3.2. Error in BP20 column for ECL models.

PREDICTED VS MEASURED:

Model type: Quad+Int

Parameter: Retention index (RI)

| | $R^2$ | Bias | RMSE | RMSE(adj) | N. Exp. | |
|---|---|---|---|---|---|---|
| 18:2 n-6 | 0.9983 | -4.663e-15 | 0.0007738 | 0.0009788 | 16 | |
| 20:2 n-6 | 0.9974 | -6.661e-16 | 0.001156 | 0.001462 | 16 | |
| 14:1 n-5 | 0.958 | -3.886e-15 | 0.0007058 | 0.0008927 | 16 | |
| 16:1 n-7 | 0.9952 | -3.553e-15 | 0.000567 | 0.0007173 | 16 | |
| 17:1 n-7 | 0.9958 | -1.776e-15 | 0.0006311 | 0.0007983 | 16 | |
| 18:1 n-9 | 0.9985 | -3.553e-15 | 0.000478 | 0.0006047 | 16 | |
| 20:1 n-9 | 0.9967 | -3.553e-15 | 0.0008813 | 0.001115 | 16 | |
| 18:3 n-6 | 0.8816 | -7.105e-15 | 0.006757 | 0.008547 | 16 | |
| 18:3 n-3 | 0.9983 | -4.441e-16 | 0.0009967 | 0.001261 | 16 | |
| 20:3 n-6 | 0.9905 | 1.11e-15 | 0.003044 | 0.00385 | 16 | |
| 20:3 n-3 | 0.9949 | -2.665e-15 | 0.001984 | 0.002509 | 16 | |
| 20:4 n-6 | 0.9977 | -4.441e-15 | 0.001941 | 0.002455 | 16 | |
| 20:5 n-3 | 0.9974 | -2.132e-15 | 0.002263 | 0.002922 | 15 | (4)* |
| Mean | 0.9846 | -2.871e-15 | 0.001706 | 0.002163 | 15.92 | |

* These programs have been excluded from the model, either because the peak did not elute, or also because of overlap in the case of EFF models.

# A3.3. Error in DB23 column for ECL models.

PREDICTED VS MEASURED:

Model type: Quad+Int

Parameter: Retention index (RI)

| | $R^2$ | Bias | RMSE | RMSE(adj) | N. Exp. |
|---|---|---|---|---|---|
| 18:2 n-6 | 0.9933 | -4.885e-15 | 0.002074 | 0.002624 | 16 |
| 20:2 n-6 | 0.9936 | -1.554e-15 | 0.002603 | 0.003293 | 16 |
| 14:1 n-5 | 0.9485 | -2.109e-15 | 0.001523 | 0.001926 | 16 |
| 16:1 n-7 | 0.9792 | -3.775e-15 | 0.00149 | 0.001884 | 16 |
| 17:1 n-7 | 0.9818 | -4.663e-15 | 0.001639 | 0.002073 | 16 |
| 18:1 n-9 | 0.9841 | -1.11e-15 | 0.001863 | 0.002357 | 16 |
| 20:1 n-9 | 0.9922 | -2.22e-15 | 0.00174 | 0.002201 | 16 |
| 22:1 n-9 | 0.9922 | -2.22e-15 | 0.002169 | 0.002744 | 16 |
| 24:1 n-9 | 0.9871 | -5.329e-15 | 0.002978 | 0.003767 | 16 |
| 18:3 n-6 | 0.9961 | -1.776e-15 | 0.002192 | 0.002772 | 16 |
| 18:3 n-3 | 0.9963 | -3.331e-15 | 0.002134 | 0.0027 | 16 |
| 20:3 n-6 | 0.9964 | -6.439e-15 | 0.002786 | 0.003524 | 16 |
| 20:3 n-3 | 0.9959 | -1.554e-15 | 0.002823 | 0.00357 | 16 |
| 20:4 n-6 | 0.9975 | -5.551e-15 | 0.002938 | 0.003716 | 16 |
| 20:5 n-3 | 0.9978 | -5.995e-15 | 0.003475 | 0.004396 | 16 |
| 22:4 n-6 | 0.9357 | -3.775e-15 | 0.01741 | 0.02202 | 16 |
| 22:5 n-3 | 0.9198 | 8.882e-16 | 0.02212 | 0.02798 | 16 |
| 22:6 n-3 | 0.897 | -7.105e-15 | 0.02778 | 0.03513 | 16 |
| Mean | 0.9769 | -3.473e-15 | 0.005652 | 0.007149 | 16 |

# A3.4. Error in BPX 70 column for ECL models.

PREDICTED VS MEASURED:

Model type: Quad+Int

Parameter: Retention index (RI)

| | $R^2$ | Bias | RMSE | RMSE(adj) | N. Exp. |
|---|---|---|---|---|---|
| 18:2 n-6 | 0.9985 | -3.331e-15 | 0.001189 | 0.001504 | 16 |
| 20:2 n-6 | 0.9983 | -6.661e-16 | 0.001592 | 0.002013 | 16 |
| 14:1 n-5 | 0.9914 | -1.665e-15 | 0.0008689 | 0.001099 | 16 |
| 16:1 n-7 | 0.9974 | -2.442e-15 | 0.0006026 | 0.0007622 | 16 |
| 17:1 n-7 | 0.9967 | -6.217e-15 | 0.0007982 | 0.00101 | 16 |
| 18:1 n-9 | 0.9974 | -6.661e-16 | 0.0008342 | 0.001055 | 16 |
| 20:1 n-9 | 0.9969 | -7.772e-15 | 0.001184 | 0.001498 | 16 |
| 22:1 n-9 | 0.9985 | -5.995e-15 | 0.0009913 | 0.001254 | 16 |
| 24:1 n-9 | 0.9986 | -2.887e-15 | 0.001176 | 0.001487 | 16 |
| 18:3 n-6 | 0.9986 | -3.331e-15 | 0.00168 | 0.002125 | 16 |
| 18:3 n-3 | 0.999 | -3.109e-15 | 0.001528 | 0.001933 | 16 |
| 20:3 n-6 | 0.9984 | -7.55e-15 | 0.00239 | 0.003024 | 16 |
| 20:3 n-3 | 0.9764 | -5.773e-15 | 0.007955 | 0.01006 | 16 |
| 20:4 n-6 | 0.9854 | -4.219e-15 | 0.01012 | 0.0128 | 16 |
| 20:5 n-3 | 0.9989 | 1.554e-15 | 0.003279 | 0.004147 | 16 |
| 22:4 n-6 | 0.9972 | -6.439e-15 | 0.004913 | 0.006215 | 16 |
| 22:5 n-3 | 0.9992 | -7.105e-15 | 0.003426 | 0.004333 | 16 |
| 22:6 n-3 | 0.9988 | -5.773e-15 | 0.004521 | 0.005719 | 16 |
| Mean | 0.9959 | -4.077e-15 | 0.002725 | 0.003446 | 16 |

# A3.5. Error in IL111 column for ECL models.

PREDICTED VS MEASURED:
Model type: Quad+Int
Parameter: Retention index (RI)

| | $R^2$ | Bias | RMSE | RMSE(adj) | N. Exp. |
|---|---|---|---|---|---|
| 18:2 n-6 | 0.9961 | -5.107e-15 | 0.003794 | 0.004799 | 16 |
| 20:2 n-6 | 0.9971 | -6.883e-15 | 0.003727 | 0.004714 | 16 |
| 14:1 n-5 | 0.9712 | -5.773e-15 | 0.004347 | 0.005499 | 16 |
| 16:1 n-7 | 0.9815 | -5.995e-15 | 0.003663 | 0.004634 | 16 |
| 17:1 n-7 | 0.986 | 2.22e-16 | 0.00354 | 0.004478 | 16 |
| 18:1 n-9 | 0.9904 | -5.773e-15 | 0.003126 | 0.003954 | 16 |
| 20:1 n-9 | 0.9838 | -5.329e-15 | 0.01364 | 0.01725 | 16 |
| 22:1 n-9 | 0.9704 | -3.553e-15 | 0.02213 | 0.02799 | 16 |
| 24:1 n-9 | 0.9985 | -4.219e-15 | 0.006016 | 0.00761 | 16 |
| 18:3 n-6 | 0.9924 | -5.329e-15 | 0.003341 | 0.004226 | 16 |
| 18:3 n-3 | 0.9974 | -1.998e-15 | 0.00446 | 0.005642 | 16 |
| 20:3 n-6 | 0.9318 | -5.551e-15 | 0.01343 | 0.01699 | 16 |
| 20:3 n-3 | 0.9981 | -1.776e-15 | 0.00451 | 0.005704 | 16 |
| 20:4 n-6 | 0.9649 | -4.885e-15 | 0.02496 | 0.03157 | 16 |
| 20:5 n-3 | 0.9986 | -4.219e-15 | 0.007011 | 0.008868 | 16 |
| 22:4 n-6 | 0.9955 | -4.663e-15 | 0.003239 | 0.004097 | 16 |
| 22:5 n-3 | 0.9985 | -1.066e-14 | 0.007913 | 0.01001 | 16 |
| 22:6 n-3 | 0.9986 | 1.554e-15 | 0.008654 | 0.01095 | 16 |
| Mean | 0.9862 | -4.441e-15 | 0.007861 | 0.009943 | 16 |